Master Course Photogrammetry and Geoinformatics

Monitoring Afforestation Areas with Earth Observation: A Case Study in Togo

Abstract

In Agou, Togo, a strategic afforestation initiative is actively restoring degraded landscapes by planting tree species. This study assesses the utility of the Normalized Difference Vegetation Index (NDVI) to monitor vegetation changes using Sentinel 2 satellite imagery from 2016 to 2024. Leveraging the capabilities of the Google Earth Engine (GEE) platform, NDVI values were processed to identify the top 95th percentile annually. The methodology extended to determining spatial correlations among vegetative covers, establishing that these were significantly clustered. A multidimensional cluster validation in R determined an optimal count of three clusters. This facilitated the implementation of a K-means unsupervised classifier that integrates NDVI-derived metrics, including trend analysis, cumulative values, and slope calculations. Additionally, assessment of regional precipitation and temperature data were incorporated into the analysis, which showed no statistically significant impacts. Our findings underscore the effectiveness of integrating remote sensing analysis and its convenience in monitoring changes in vegetation land cover.

Keywords: GEE, Change vegetation, R, NDVI, afforestation, k-means, Spatial correlation

Table of Content

Abstract **3**

Table of Content **4**

Table of Figures **5**

Table of Tables **6**

Table of Equations **7**

Abbreviations **8**

1 Introduction **9**

2 Theoretical Background and Related Research **10**

3 Objectives **10**

4 Methodology **22**

4.1 Case of study TOGO project description 23

4.2 Datasets 24

4.3 Data Processing 24

4.4 Spatial Analysis 25

4.4.1 NDVI Trend Analysis 25

4.4.2 NDVI cumulative 26

4.4.3 Spatial autocorrelation analysis 26

4.4.4 Clustering of vegetation gain 27

4.5 Other statistical analysis 28

4.6 Validation with field data 28

5 Results and discussion **29**

5.1 NDVI interpretation and analysis 29

5.2 Spatial correlation 34

5.3 Clusters 35

5.4 Impact of Climatic Factors on NDVI 39

5.5 Final interphase users 40

5.6 Field validation of cluster outcomes 42

6 Conclusions **46**

7 Recommendations for future research **48**

References **49**

Table of Figures

Figure 1. Workflow of methodology. 22
Figure 2. General Location of TOGO project areas 23
Figure 3. NDVI time series from 2016 – 2024, Abudjokopé zone. 30
Figure 4. NDVI time series from 2016 - 2024, Fokpo zone. 30
Figure 5. Mean NDVI from 2016 to 2024 in the study area 32
Figure 6. NDVI metrics in Fokpo. 33
Figure 7. NDVI metrics in Abudjokopé. 34
Figure 8.The best number of clusters by R version 4.4.2. 35
Figure 9. Graph of the best number of clusters by R version 4.4.2. 36
Figure 10. Classification of clusters. 38
Figure 11. Classification in Abudjokopé. 38
Figure 12. Classification in Fokpo. 39
Figure 13. User interface of GEE cluster algorithm for TOGO project study area. 41
Figure 14. Legend of layers map display 42
Figure 15. Distribution of trees by Cluster category 44

Table of Tables

Table 1. Sentinel 2's Bands Information. 12
Table 2. Sample trees by Cluster category. 43
Table 3. Physical characteristics of trees average by Clusters. 43

Table of Equations

Equation 1. Normalized Difference Vegetation Index..24
Equation 2. Linear regression...26

Abbreviations

EVI	Enhanced Vegetation Index
GEE	Google Earth Engine
GIS	Geographical Information System
FVC	Fractional Vegetation Cover
IDE	Integrated Development Environment
IPCC	Intergovernmental Panel on Climate Change
MSI	Multi-spectral Instrument
NDVI	Normalized Difference Vegetation Index
NIR	Near-Infrared
SAVI	Soil-Adjusted Vegetation Index
SEO	Satellite Earth Observation
SWIR	shortwave infrared
UNCCD	United Nations Convention to Combat Desertification
UNFCCC	United Nations Framework Convention on Climate Change
VNIR	Near-infrared

1 Introduction

The critical role of reforestation in addressing global environmental challenges, including climate change mitigation, biodiversity conservation, and the restoration of degraded ecosystems, (Intergovernmental Panel On Climate Change (IPCC), 2023).In Togo, a country significantly affected by deforestation due to agricultural expansion, logging, and other anthropogenic activities , reforestation initiatives are critical to promoting sustainable land management and ecological recovery (Dembner et al., 1994)(UNEP, 2019). The case study, set in Togo, details deforestation and forest cover loss in the early 2000s, and subsequent afforestation activities started by Nature Office in 2012. This initiative focused on the planting of native tree species, with the aim of establishing a nature conservation area.

The success of these initiatives depends on the mapping, monitoring and assessment of forest cover. Considering the impact and continuous change of forest ecosystem conditions due to anthropogenic activities. Satellite Earth Observation (SEO) mapping at different scales using geospatial platforms such as Google Earth Engine (GEE), with access to large spatial data sources and high computing power, is expected to enable efficient and accurate monitoring of vegetation dynamics in defined areas of interest (Kovyazin et al., 2023). The integration of optical satellite imagery with index interpretation allows vegetation dynamics to be monitored efficiently (Gamon et al., 1995) (Wagenseil & Samimi, 2006), and information provided to stakeholders.

This proposed study aims to develop a geospatial tool to identify areas of vegetation change resulting from reforestation activities conducted by NatureOffice in Togo. Utilizing Sentinel 2 and GEE optical satellite imagery, the tool focuses on assessing vegetation recovery in designated impact areas. Normalized Difference Vegetation Index (NDVI) metrics, temporal trends, and spatial clusters will be employed to identify and quantify vegetation transitions between 2016 and 2024, the available timeframe for these optical data. The results will highlight areas that may serve as revisit points for project implementers to identify significant increases in forest cover over time.

2 Objectives

The objective of the present research is to develop a geospatial tool employing Google Earth Engine (GEE) for analyzing optical satellite imagery (i.e., Sentinel 2) and vegetation indices to assess areas of progress in reforestation activities in a case study in Togo.

The following specific objectives will be considered:

- To calculate the Normalized Difference Vegetation Index (NDVI) across the entire dataset of Sentinel-2 imagery from 2016 to 2024 through an online platform GEE to establish a comprehensive baseline of vegetation health and dynamics.
- To analyze NDVI values from Sentinel-2 optical satellite imagery to specifically assess changes in vegetation within designated afforestation areas from 2016 to 2024, identifying regions of significant reforestation progress or decline.
- To employ statistical clustering and unsupervised classifier techniques on NDVI images to discern, categorize, and analyze temporal and spatial vegetation patterns within the afforestation project areas, aiding in the evaluation of reforestation efficacy over time.

3 Theoretical Background

This section of the thesis provides a comprehensive overview of the theoretical foundations and technological advances underpinning modern remote sensing techniques. It explores essential topics that provide a comprehensive theoretical framework for understanding the scope of the study, detailing the technological tools, datasets, and spatial analysis processes essential to this research. By highlighting the integration of these elements to facilitate advanced environmental monitoring and analysis, this section serves as a foundation for further exploration of the specific methodologies and applications employed in the study.

3.1 Remote Sensing

The development of satellite sensors for remote sensing has undergone significant advancements, characterized by variations in sensor aperture types—synthetic or optical—as well as differences in quality, resolution, and the range of spectral responses. The advancements have revolutionized the technological ability to capture and analyze information on the Earth’s surface. (Han et al., 2022). The distinction among the components is derived from the unique spectral reflectance characteristics of the captured objects. Each component interacts with various segments of the electromagnetic spectrum due to its specific physiological and biochemical properties. Optical sensors have the ability to discriminate objects over a wide range of real-world scenarios and spatial scales. The diverse spectral responses of optical sensors allow detailed information to be extracted, making them essential tools in a variety of fields; the applications encompass a range of domains, including Urban Planning, Supporting infrastructure mapping and analysis, Agriculture, Monitoring crop health, and estimating yields.; Environmental Monitoring: Identifying changes in vegetation cover and assessing water quality; Disaster Management: Evaluating damage and aiding response efforts.(Schowengerdt, 2007)

The capacity to capture data across the extensive electromagnetic spectrum is influenced by the physiological and biochemical characteristics of objects, such as chlorophyll content, water composition, and cell structure. Below are the primary characteristics of vegetation that respond to different electromagnetic spectrum ranges.

Visible Spectrum (400–700 nm): Vegetation demonstrates strong absorption in the blue (450–495 nm) and red (620–750 nm) bands due to the presence of chlorophyll while reflecting green light (495–570 nm), which explains its green appearance.

Near-infrared (700–1,300 nm): This region is characterized by a strong reflectance caused mainly by light scattering in the spongy cells of the leaf mesophyll. The spectral response is sensitive to the vegetation's structure, making it critical for monitoring biomass and canopy density.

Middle-Infrared (1,300–2,500 nm): Reflectance is sensitive to vegetation water content and health. Strong water absorption bands are observed at 1,450 nm and 1,950 nm, while reflectance peaks between 2,000 nm and 2,500 nm are associated with leaf stress and structural variations. (Guyot et al., 1989)

Sentinel 2

The sentinel-2 multi-spectral instrument (MSI) imagines mission with the European Space Agency's Copernicus Program, which is designed for monitoring and environmental management. This is a twin satellite flying in the same orbit but phased at 180° that includes Sentinel-2A and Sentinel-2B in high-resolution optical imagery with a revisit of 5 days at the equator. Sentinel-2A was launched in June 2015, followed by Sentinel-2B in March 2017, marking a significant advancement in Earth observation capabilities.

The Sentinel-2 Multi-Spectral Instrument (MSI) is equipped with 13 spectral bands, covering the visible, near-infrared (VNIR), and shortwave infrared (SWIR) regions of the electromagnetic spectrum, delivering imagery at three spatial resolutions including four bands at 10 m, six bands at 20 m, and three bands at 60 m spatial resolution tailored to different application. With an orbital swath width of 290 km, Sentinel-2 enables efficient large-scale monitoring, supporting a wide range of environmental and ecological studies (European Space Agency et al., 2024), detailed information is displayed in the following table:

Table 1. Sentinel 2's Bands Information.

Band Name	Spatial Resolution (m)	Central Wavelength (nm)	Bandwidth (nm)	Description
Band 1	60	443	20	Aerosol detection and coastal water monitoring
Band 2	10	490	65	Blue, is useful for water quality and bathymetry
Band 3	10	560	35	Green, for vegetation monitoring and water bodies
Band 4	10	665	30	Red, for vegetation discrimination and chlorophyll
Band 5	20	705	15	Red-edge 1, for vegetation monitoring
Band 6	20	740	15	Red-edge 2, for chlorophyll absorption
Band 7	20	783	20	Red-edge 3, sensitive to biomass and leaf structure
Band 8	10	842	115	Near-Infrared (NIR), for vegetation vigor
Band 8A	20	865	20	NIR narrow, for improved vegetation monitoring

Band 9	60	945	20	Water vapor absorption
Band 10	60	1,375	30	Cirrus cloud detection
Band 11	20	1,610	90	SWIR1, for vegetation moisture and soil properties
Band 12	20	2,190	180	SWIR2, for snow, ice, and burned area mapping

3.2 Land Cover Detection Using Satellite Imagery

Remote sensing allows for creating thematic maps representing land cover, which can be derived from various types of satellite data. Common techniques focus on the use of high-resolution multispectral and hyperspectral imagery, which significantly enhances the accuracy of object detection and the characterization of surfaces. (Foody, 2002)

Thematic mapping is typically performed through techniques that rely on either a visual analysis or automated analysis. These methods have been developed through the use of visual analysis, which relies on the human eye to interpret data through visual cues, and automated analysis, which utilizes algorithms and computational techniques to identify and categorize information by supervised or unsupervised classifiers.(Congalton, 2001) Classifiers work by grouping pixels based on detected patterns, shapes, spectral similarities, or combinations of these elements to identify predefined spectral signatures or patterns. The development of algorithms designed to exploit the spectral and radiometric characteristics of images has led to substantial advancements in both supervised and unsupervised classification methods. Supervised classification techniques require labeled data for training models, enabling precise identification and categorization. In contrast, unsupervised classification identifies patterns and clusters within data without the need for predefined labels. (Lu & Weng, 2007) These developments highlight the transformative impact of computational innovation in land cover detection and thematic mapping,. They emphasize that thematic mapping aims to be an analytical and reliable process, which relies on the collaborative efforts of processing data sources, planning visual identification, managing resources, and selecting the final map outputs.

3.3 Vegetation Indices

Satellite sensors detect red and near-infrared light waves reflected from the Earth's surface by recording them in specific spectral bands. By applying mathematical formulas and algorithms, these light wave values create an indicator of vegetation cover, represented as a pixel value. Various vegetation indices have been developed using combinations of satellite image bands to emphasize vegetation responses across two or more spectral bands. The analyzed responses are then summarized into a single value, providing useful information about vegetation. (Zoran, 2007)

A vegetation index is a statistical model component used to estimate regional vegetation. The indices are designed to maximize sensitivity to vegetation characteristics and the particular biophysical phenomena.("Estimate of Vegetation Production of Terrestrial Ecosystem," 2020) . These indices are critical for estimating biophysical variables across diverse ecosystems, including vegetation density, productivity, and water content. (Xue & Su, 2017). Indices that provide a description of vegetation behaviour can be:

- **Normalized Difference Vegetation Index (NDVI)**: Utilizes the near-infrared (NIR) and red bands of optical sensors to calculate vegetation cover. NDVI values range from -1.0 to +1.0, where values below 0.5 indicate sparse vegetation and values above 0.5 signify dense vegetation. This index is sensitive to green vegetation and is widely used to assess vegetation health and density.
- **Soil-Adjusted Vegetation Index (SAVI)**: Designed to minimize the soil background influence on NDVI by incorporating a soil brightness correction factor (L), typically set at 0.5. This makes SAVI particularly useful in arid and semi-arid areas where exposed soil can affect the NDVI readings. SAVI helps provide more accurate measurements of vegetation cover in these regions.
- **Enhanced Vegetation Index (EVI)**: Aims to optimize the vegetation signal with its formulation that corrects for atmospheric conditions and soil background. It uses NIR, red, and blue spectral bands and includes coefficients to reduce aerosol influences, making it suitable for areas with high biomass. EVI is helpful in reducing saturation effects that can occur with NDVI in dense vegetation areas.

3.4 Geographic Information Systems (GIS) and Geospatial Platforms

A Geographic Information System (GIS) is a computer system designed to analyze and display geographic information located in a coordinate reference system(U.S. Geological Survey & U.S. Department of the Interior, 2024). Technological advances have facilitated the migration of Geographic Information Systems (GIS) management infrastructure from traditional methods to desktop software and online platforms. These platforms and software enable the creation, management, analysis and mapping of diverse datasets.

The utilization of Geographic Information Systems (GIS) facilitates a comprehensive understanding of geographic data by identifying patterns, relationships and contexts. This capacity enhances communication, efficiency, management and decision-making processes across a range of multidisciplinary domains.(ESRI, 2024) Advancements in GIS have culminated in the establishment of this technology as a pivotal instrument for addressing intricate spatial and thematic challenges.

Software can be found in both commercial and non-commercial versions. Commercial software requires a fee or research account to access the elements and tools developed to analyze geospatial data efficiently and accurately. Commercial and non-commercial software is available. For access to the environment, elements and tools developed for efficient and accurate analysis of geospatial data, commercial software requires payment of a fee or a research account for access, and non-commercial software is available online with no access restrictions, but with limitations on advanced functions in a practical approach.

ArcGIS Pro: It is a comprehensive commercial desktop and online GIS software designed to enable users to explore, visualize, and analyze data across 2D maps, 3D maps, and 4D scenes. The software provides an intuitive user interface, facilitating efficient data management, analysis, and the display of results. Additionally, it offers advanced tools and capabilities, empowering users to perform complex spatial analyses and effectively support their workflows.(Esri, 2024)

QGIS: It is a comprehensive non-commercial desktop GIS software designed and developed on free and open-source.It is designed to facilitate the creation of high-quality cartographic outputs and conduct advanced geospatial analysis. QGIS offers an extensive toolset, automated workflows, and support for third-party plugins, allowing users to perform a wide range of geospatial operations. Additionally, it is highly interoperable, enabling seamless integration with other platforms, databases, and visualization tools. Its flexibility and robust capabilities make it a valuable resource for researchers, educators, and practitioners across diverse fields. (QGIS Development Team, 2024)

Google Earth Engine (GEE): Google Earth Engine is designed for scientific analysis and visualization of geospatial data. It hosts a multi-petabyte catalog of satellite imagery and other geospatial datasets, enabling users to access, process, and analyze vast amounts of data efficiently. The platform integrates application programming interfaces (APIs), libraries, and workflows that facilitate the seamless processing and management of geospatial data. This infrastructure allows for the implementation of advanced analytical workflows, including large-scale temporal and spatial change detection, spanning decades of historical and contemporary satellite observations, unparalleled processing power for the analysis of complex algorithms across spatial and temporal dimensions.

The platform is freely accessible for non-commercial use by researchers, nonprofits, educators, and governmental agencies to analyze large-scale geospatial data; other uses can be commercial or operational applications. Access is provided under specific licensing agreements.(Gorelick, N. et al., 2017)

Both commercial and non-commercial GIS software have the capacity to work in conjunction with remote sensing or spatial data storage platforms through the use of tools or extensions that connect to the database. This facilitates more efficient and practical data processing, whether accessed from desktop or online software. The nesting of such software does not limit or reduce the quality of the information accessed and allows the user to manage and analyze large amounts of data using the available tools.

3.5 Statistical software

Statistical software is specialised software designed to facilitate the processing, analysis, interpretation and visualisation of data. The tools include a wide range of statistical methods, from the most basic to advanced techniques, with which users can obtain accurate and precise results depending on the selection and configuration of the libraries and model parameters used. RStudio, a free software integrated development environment (IDE) for the R language, provides graphics and statistical computation. (R Core Team, 2020) The practical user interface and the extensive online collection of libraries and scripts facilitate the use of the code editor, data visualization, and analysis capabilities in versatile environments such as academic, industrial, and research applications.

3.6 Afforestation and restoration activities

Afforestation is defined as a human intervention to convert land that has not been forested for a long period of years into the forest through activities of planting and seeding to induce the promotion of natural seed sources.

Reforestation refers to the re-establishment of forests in areas where forests previously existed. This process often involves replacing the previous crop with the same or different species, depending on ecological and management objectives.(Barthlott et al., 2009)

Restoration is defined as the accompanying increase in structure and function promoted by human interventions, paralleling the changes that occur during secondary succession.(Cortina et al., 2006)

These activities are a direct response to the increasing rates and impacts of deforestation, which continue to rise due to growing pressure to extract primary resources and clear land for economic development activities. Afforestation, reforestation, and restoration serve as viable alternatives to recover land cover and improve ecosystem health. The efforts integrate strategies to revive biodiversity and restore ecological functions, which are essential for the livelihoods of rural communities that depend on these ecosystems.(Lamb et al., 2005)

4 Relate research

4.1 Related research about land cover detection by vegetation indexes

Remote sensing technologies and geo-analytic platforms have revolutionized multi-purpose spatial analysis over time, improving the methods of acquiring spatial imagery through different types of satellites and resolutions. In the context of land cover analysis, the provision of scalable and multi-temporal solutions for assessing land cover and ecosystem change. Leveraging satellite imagery and indices generated by the use of image bands, the vegetation index had improved the detection of vegetation and its characteristics that can be detected such as health, changes, water content and expansion. The use of multi-operational geospatial platforms enhanced these capabilities by providing access and manipulation of large datasets on computational power large-scale analyses. This section reviews and provides insight into the key studies demonstrating the interoperability of satellite imagery, vegetation indices, and geospatial platforms can provide reasonable results on vegetation landcover analysis.

4.2 Monitoring vegetation using satellite imagery

Vegetation phenology is highlighted as a main indicator of how the ecosystem responds to the environment, manifesting growth patterns, behaviour, physical activity, and sensitivity to climate variations. (Jin & Eklundh, 2014) . There is ample evidence that the phenological phenomena of vegetation manifest regular cycles observable in various contexts. These include the appearance of buds, the unfolding of leaves, changes in forest flora, and the cycles of sprouting and maturation of agricultural crops (De Beurs & Henebry, 2005) (Zeng et al., 2020) . The observation of phenological stages can be detected from visual interpretation, near-surface measurements, and spatial analysis. (Zeng et al., 2020).

Spatial observations provide information on vegetation phenology based on remotely sensed models, as evidenced by the surface observations derived from the wavelengths and spectral reflectivity of the multiband sensor. (Yang et al., 2017) Satellite-based remote sensing offers methodologies provides a comprehensive, global perspective on phenological phenomena, thus facilitating comprehensive research at large scales. (Zhang et al., 2006)

Sensors as Sentinel 2 with a constellation of two satellites that provides free publicly-accessible high-resolution optical imagery at 10–60m resolution at a 5 day interval (Liu et al., 2017). These Sentinel-2 satellites provided a precisely calibrated measurement system overcame the spatiotemporal limitations of current satellite sensors and showed their potential in ongoing phenological studies.(Vrieling et al., 2018)

Indexes of vegetation are widely used for phenology characterization (Rouse, 1973), particularly the Normalized Difference Vegetation Index (NDVI), considering the calculation using red band is sensitive to chlorophyll pigment content and near-infrared is sent to internal leaf structure capture typically in spectral bands of optical sensors. (Zeng et al., 2020) (De Beurs & Henebry, 2005). The most common use of remote sensing visual interpretation included the NDVI for vegetation detection (Wagenseil & Samimi, 2006), and time series highlights the evolutionary growth from a lower to a higher NDVI value, considering the atmospherically corrected surface, which minimizes the significant variability between spatial image captures.(Houborg & McCabe, 2018) The researchers use the index at regional and global vegetation validation to show the canopy structure and leaf area per unit ground on the remote detection of fluorescence directly related to the efficiency of photosynthesis (Gamon et al., 1995) (Grace et al., 2007)

Apart from NDVI, the EVI has been investigated for vegetation monitoring because of its ability to account for spectral behavior, in particular, its increased dependence on near-infrared (NIR) reflectance. EVI demonstrates improved performance by compensating for variations caused by changes in the solar zenith angle (SZA), ensuring more accurate tracking of vegetation in varying illumination conditions and minimizing the impact of shadowing, which increases with forward scattering and decreases with backscattering (Galvão et al., 2013) .As given the NDVI presents some shortcomings in describing the associated behaviour between the vegetation and soil spectral response (A. R. Huete, 1988). Another index the SAVI has been evaluated in various studies focusing on the detection and effects on vegetation (Qi et al., 1994) (Ren et al., 2018) (Zhen et al., 2021), the studies have shown an improvement in the sensitivity of perceiving the soil background through the use of the L factor, which is linked to the degree of vegetation coverage (Major et al., 1990). The index performs best when analyzing cases with high canopy density and extensive coverage. Its implementation significantly enhances the results, creating distinct spectral signatures between vegetation and soil, bare soil, and non-vegetative covers.

Based on the vegetation index analysis on remote sensing, the NDVI has been considered a confident and accurate method of detecting vegetation and phenology if considerations such as atmospheric surface correction were implemented(Xue & Su, 2017). Used in time series reasoning of NDVI results per pixel in a study area, it provides a decreasing, increasing, or fluctuating trend that allows the interpreter to understand the recorded behaviour. In recent decades, it has been the main indicator of vegetation land cover loss caused by direct anthropogenic impact, natural disasters or climate change.

The land cover change is considered a high component in the climate change that affected the ecologic system. (Vitousek, 1994). The interpretation of cover over time reveals the complex conditions of temporal and spatial data variability. This is a pivotal aspect of the multi-seasonal information found in time stacks of imagery (Schneider, 2012).

4.3 Integration of Google Earth Engine (GEE) for Forest Monitoring

The integration of geospatial analysis platform, data access sources online and vegetation indexes has significantly enhanced the ability to monitor and detect vegetation dynamics over the time. The platform of GEE stands out as a compelling geospatial tool for processing satellite data, simplifying the large scale, multi temporal and spatial resolution. The satellite imagery indices present a robust approach for tracking vegetation and mapping land cover use over time using the online platform (Amiri & Pourghasemi, 2022).

A case of use of Landsat imagery to analyze land-use and land-cover changes in northern Togo's protected areas from 1987 to 2007 evaluated the changes through the NDVI and subsequences supervised classification including seven classes which results on an overall of 72% accuracy, the research yielded several noteworthy findings, with the most salient ones manifesting between 200 and 2007. These findings emerged as a consequence of the spectral homogeneity among classes. (Folega et al., 2014) . A comparable investigation of Central Africa employed MODIS imagery and NDVI time series data to assess forest dynamics. The study concentrated on seasonal vegetation fluctuations and multi-annual availability. The research indicated a propensity for the annual green response to phenological alterations to occur during peak times. The analysis evaluated the precipitation, finding no significant impact on the local scale. The woody plant encroachment due to increased moisture was also assessed. The results furthered understanding of the complex interaction of ecological and spatial variability in savanna interannual vegetation. (Wagenseil & Samimi, 2006)

Dynamic forest monitoring requires diverse input data and complex processing methods to achieve accurate assessments. In a study conducted in Kon Tum Province, Vietnam, Kovyazin et al. (2023) implemented a forest monitoring methodology on the cloud-based platform Google Earth Engine (GEE). In using GEE, the study addressed the remaining challenges related to cloud cover, atmospheric conditions and sensor limitations, which are common factors affecting the reliability of the results obtained. The integration of NDVI and machine learning algorithms enabled the detection of forest changes in the study area. However, the research was mainly focused on a specific time frame, which may have limited its ability to capture longer-term trends and dynamics. Despite these limitations, the study demonstrated the potential of GEE as a robust platform for processing multispectral data and monitoring forest cover change with high computational efficiency (Kovyazin et al., 2023).

4.4 Afforestation and Reforestation Projects

The degradation and deforestation of land cover are associated with anthropogenic impacts, it have accelerated the loss of vegetative cover and ecosystem health on global scale. Activities identified as primary factors are agricultural frontier expansion, forest logging, urbanization, and development areas among vegetation forest cover. These activities often result in fragmented landscapes, biodiversity impacts, water availability, disruption of ecosystem services, food security and quality of life of stakeholders (Geist & Lambin, 2002). For instances, wildfires on central Brazilian Amazon occurred only in years of extreme drought induced by El Niño, on particular areas close to land and water communication routes being attractive for active agriculture and pasture aim of livestock (Dos Reis et al., 2021). Other research presents the expansion of soybeans into pastures as an another caused, it was initially observed between 2000 and 2019, with the area under soybean cultivation increasing more than twice from 26.4 Mha to 55.1 Mha, using a satellite-based analysis for mapping (Song et al., 2021). Moreover, the demand for timber products has led to unsustainable levels of timber harvesting, which is a significant factor in the observed change in land use patterns in tropical countries such as Nigeria, the Philippines, Benin, Ghana, Indonesia, Ecuador, Costa Rica, Brazil and others (Goldman & Weisse, 2024)(Anna, 2024). The presented case-studies provide an insight into the relevance of monitoring affected areas and thereby underscore the importance of effecting action in these areas. The underlying objective of the green initiative is to address or counteract the adverse impact of these conditions.

Green projects encompass activities such as afforestation, restoration, and reforestation in affected regions. The utilization of technological remote sensing studies, which have been employed in practical applications of GEE extend beyond research to include the FAO's collect earth initiative offers the possibility to undertake monitoring tasks by assess their Land use, land-use change, and forestry processes and to report to the United Nations Convention to Combat Desertification (UNCCD) and United Nations Framework Convention on Climate Change (UNFCCC)(Saah et al., 2019) (FAO, 2025).

A study leveraging the Normalized Difference Vegetation Index (NDVI) within the GEE platform successfully demonstrated the effective of afforestation areas by examining temporal changes in vegetation indices. The research proposed an adaptive detection algorithm to identify afforestation planting times based on abrupt increases in NDVI trends on Landsat imagery. The analysis focused on the middle section of the Yangtze River (YZR) Valley from 1988 to 2020, mapping the spatial and temporal distribution of afforestation projects. The results indicated a concentration of early afforestation efforts along the southern coast of the YZR. The study concluded that this method effectively mitigates disturbances caused by atypical and afforestation conditions, providing an accurate and scalable approach to track afforestation trends over time.(Fu et al., 2021)

In an alternative study using MODIS 3Q1 data in GEE to analyse the spatial and temporal changes of vegetation cover in the Three North China Forest Protection Project area between 2000 and 2020, researchers estimated fractional vegetation cover (FVC) using a dichotomous image element model that ensures high data reliability by correcting for atmospheric disturbances such as water, clouds, heavy aerosols and cloud shadows. The results indicated a significant increase in FVC across the two-decade period, with an expansion of medium and high vegetation cover areas. In particular, the FVC of tall vegetation increased from 20.66% in 2000 to 21.59% in 2020, indicating increased vegetation activity. The study further noted a strong positive correlation between vegetation cover and precipitation, especially in mountainous regions with minimal human interference. In contrast, in the lowlands, where humans intervention are more common, irrigation played a crucial part in shaping vegetation dynamics.(Li et al., 2023)

5 Methodology

The section details into the comprehensive spatial analysis conducted to evaluate the vegetation dynamics within the study area. Employing the spatial analysis tool of the Google Earth Engine (GEE), this section outlines methodologies ranging from trend analysis using NDVI data to evaluation of external factors that may influence NDVI results with R studio and clustering techniques. The analysis aims to uncover temporal changes, assess the spatial autocorrelation of vegetation patterns, and classify the landscape into vegetative change zones, as the diagram shows.

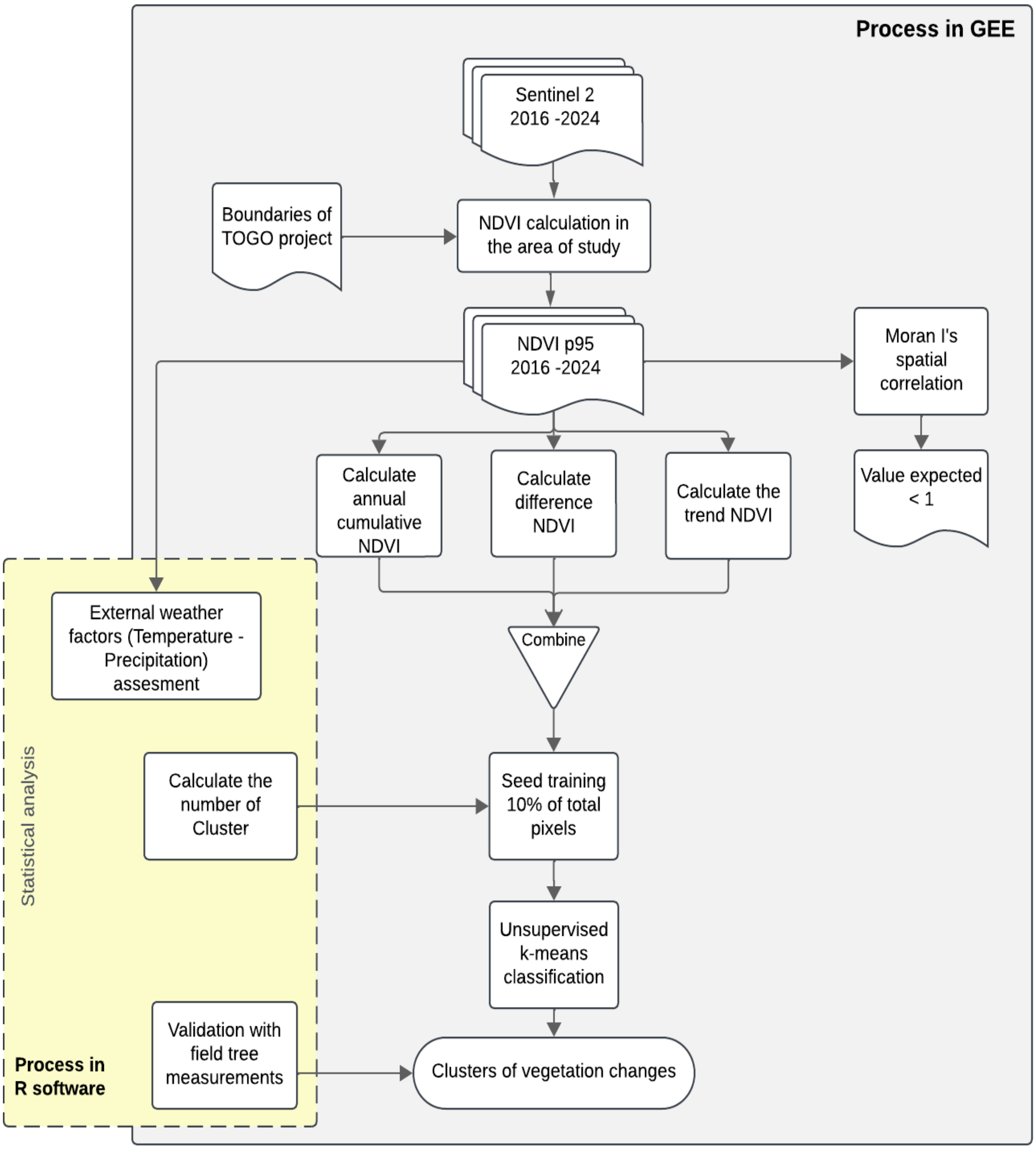

Figure 1. Workflow of methodology.

5.1 Case of study TOGO project description

The Nature Office's Named Togo project focuses on CO2 sequestration through natural forest afforestation in degraded areas by planting native trees and other social and sustainability initiatives that improve the livelihoods of local people. These activities started in 2012 and continue to the present day, focusing on two areas, mainly Fokpo in the northwest of Agou and Abudjokopé in the southeast. (natureOffice, 2025)

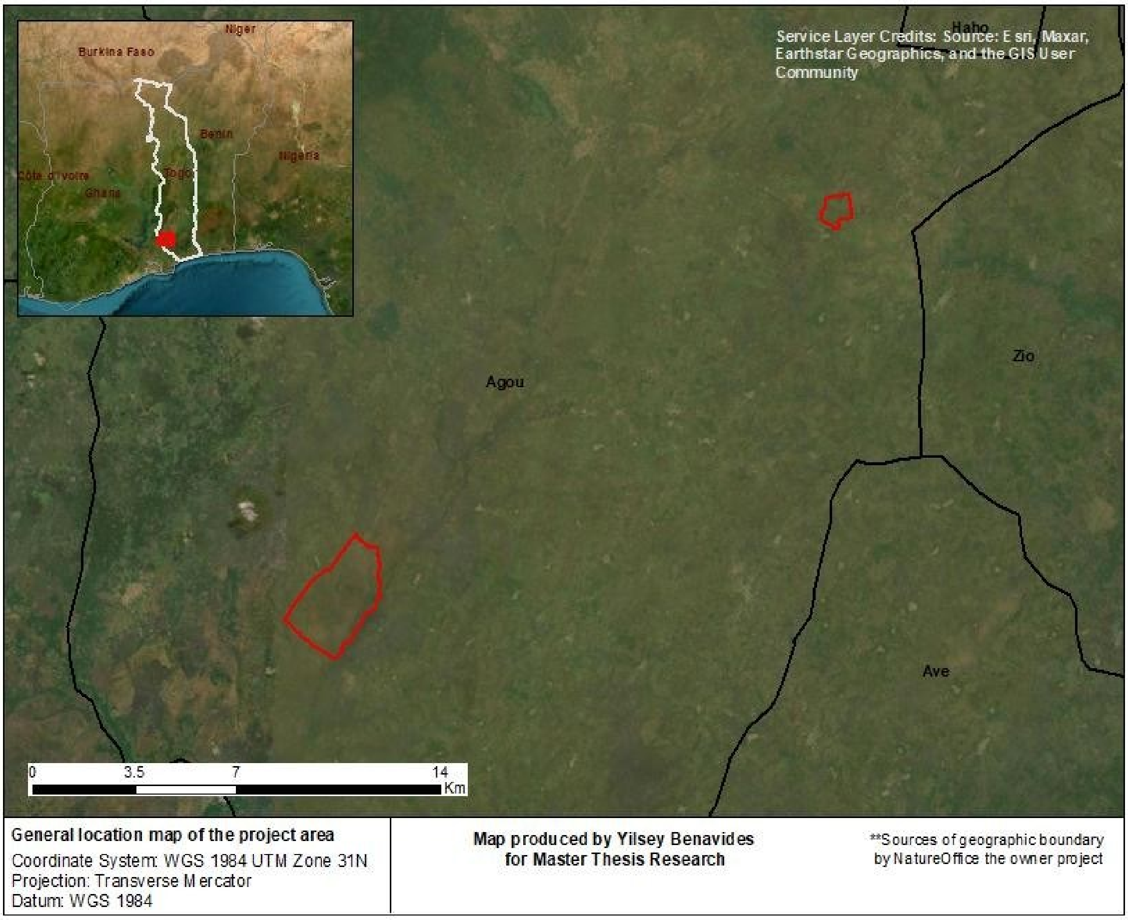

Figure 2. General Location of TOGO project areas.

The study was carried out in the Plateaux region, Préfecture of Agou in Togo. The area is part of the Guinean forest-savanna ecoregion, which features a mixture of dense natural forest, tropi- cal moist forest, grassland, and savanna landscapes, particularly in West Africa (Olson et al., n.d.). The region's climate is humid due to its tropical location, with average temperatures rang- ing from 25° to 27°C. It receives approximately 1,200 mm of precipitation annually. (The World Bank Group, 2021) Agou is distinguished by its high biodiversity, encompassing a vari- ety of plant species from towering hardwood trees to a wide array of shrubs and herbaceous plants. This rich flora supports a diverse fauna, including numerous species of mammals, birds, reptiles, and insects. The biodiversity and dynamic interaction between diverse ecosystems facilitate ecological balance and support food supplies, making the Guinean savannah a critical area for conservation efforts. (Bongers et al., 2005)

5.2 Datasets

Datasets of multispectral imagery from the Sentinel-2 satellite, operated by the European Space Agency (ESA). Details about the satellite's capabilities and its role in environmental monitoring are extensively discussed in the section Theoretical Background and Related Research 10.For the study purpose, the 10-meter spatial resolution bands, incorporating radiometric and geometric correction, in L2A products provide surface reflectance values that ensure the data accurately reflect surface features by removing atmospheric influences such as aerosols and other particulates (European Space Agency et al., 2024).

5.3 Data Processing

The Sentinel-2 dataset imagery was the primary source of the analysis. This one was used as inputs for the NDVI identified and discriminated vegetation biomass and health by comparing the differential reflectance of near-infrared (NIR) and visible red light (Freden, S. C. et al., 1974). This index is particularly sensitive to chlorophyll presence in vegetation, making it an effective tool for assessing changes in plant health over time. (Xue & Su, 2017)

The most widely used is the Normalized Difference Vegetation Index (NDVI), it was proposed by Rouse Jr. et al., (Freden, S. C. et al., 1974)

Equation 1. Normalized Difference Vegetation Index

$$NDVI = \frac{(\rho_{NIR} - \rho_{Rred})}{(\rho_{NIR} + \rho_{Rred})}$$

$\rho_{NIR} = Near\ Infrarred\ band\ of\ the\ optical\ sensor$

$\rho_{RED} = Red\ band\ of\ the\ optical\ sensor$

The vegetation index used the reflectance for visible (ρRED) and near-infrared (ρNIR) radiation of spectral bands for calculation (Choudhury, 1987), and resulting in values of the index ranging from -1.0 to +1.0, displaying the healthier and present vegetation. The scale used to determine vegetation cover ranges from 0, representing an area with minimal vegetation cover, to below 0.5, indicating sparse or moderately light vegetation, and above 0.5, the scale denotes an area with dense and continuous vegetation.

This index demonstrates significant sensitivity to green vegetation, including in areas with minimal vegetation cover. Consequently, it has been adopted in research on the structure and density of vegetation coverage.(Xue & Su, 2017)

It is acknowledged that data availability for Sentinel 2 is only available after 2015. Therefore, the time period 2016 to 2024 was selected by creating annual NDVI images using the highest quality pixel values (95th percentile) within the annual data composite. This approach minimizes the impact of atmospheric perturbations, such as cloud cover and aerosols, and ensures that only the most reliable data are considered in the analysis. Selecting the 95th percentile of the dataset maintains consistency between the availability of imagery each year and its evaluation, allowing for a less biased interpretation of the timeframe within each year and enhancing the temporal trends of vegetation dynamics in the study area, all conducted using the GEE platform.

5.4 Spatial Analysis

This section outlines the spatial analysis methodology used in studying vegetation dynamics within the designated study areas. This methodology is crucial for understanding vegetation distribution and health, as it provides essential information on spatial patterns and ecological processes through accurate vegetation cover mapping and analysis of its changes over time. This will aid in identifying areas of significant ecological interest, such as regions with high vegetation density, areas undergoing substantial transition, and areas impacted by environmental restoration factors.

NDVI Trend Analysis

To assess temporal changes in vegetation over time in the designated study areas, the Google Earth Engine (GEE) platform played a crucial role in facilitating the primary data processing tasks. For this purpose, an academic account was created to access the platform, leveraging the extensive tools, libraries, big data access, and functions provided by GEE. Utilizing the previously mentioned data sources as assets, linear regression analysis was conducted on annual NDVI data derived from Sentinel-2 imagery spanning from 2016 to 2024.

Linear regression is employed to predict a dependent variable (Y) based on one or more explanatory variables (X). The following equation expresses the model:

Equation 2.Linear regression

$$Y = \beta_0 + \beta_1 X_1 + \beta_2 X_2 + \cdots + \beta_n X_n + \in$$

Where:

β_0 = is the intercept,

$\beta_1, \beta_2, \ldots, \beta_n$ = are the coefficients of the independent variables,

$X_1, X_2, \ldots, X_n$ = are different independent variables that influence,

$\in$ = is the error term,

This model describes this relationship through a function that explains and predicts the target variable's values based on the predictors. (Tjøstheim et al., 2022) This method quantifies the rate and direction of vegetation changes based on the annual NDVI values, revealing whether vegetation health is improving, degrading, or remaining stable. This analytical approach is fundamental in understanding the ecological dynamics within the study area, providing insights essential for effective environmental management and conservation efforts.

NDVI cumulative

In order to provide further validation of the spatial trend analysis of NDVI behavior over time, the cumulative NDVI change analysis was employed. This approach offers a comprehensive evaluation of both temporal and spatial patterns in vegetation cover, responding dynamically to varying ecological conditions. Analysis of this kind aids in tracking changes related to degradation and fragmentation, which have the potential to be linked to adverse impacts on the environment.(Pettorelli et al., 2005). The approach integrates annual NDVI values from 2016 to 2024 for each pixel within the designated study areas. This methodological approach, executed within the GEE platform, is calculated by summing normalized NDVI values on an annual basis through the application of a step-down function. This function helps to identify general trends in vegetation growth or decline over time in critical regions.

Spatial autocorrelation analysis

Spatial autocorrelation refers to the presence of systematic spatial variation in a mapped variable, and is distinguished by contrasting values in the observations. In instances whereby observations exhibit significantly divergent values, the cartographic representation exhibits negative spatial correlation, contrasting with positive results that suggest spatial correlation. A range of techniques exists for detecting correlation within a spatial distribution of values. These correlations are typically interpreted as indicators of intriguing phenomena within the distribution of map values, necessitating further exploration to comprehend the underlying causes of observed spatial variation and implying information redundancy. (Smelser & Baltes, 2001)

Moran's I univariate traditional statistic was used to assess the spatial patterns of NDVI values across the study area. This statistical measure helps identify the degree to which similar NDVI values are clustered or dispersed across the landscape, offering insights into spatial dependencies and potential ecological processes influencing these patterns.(Yamada, 2024). The platform GEE platform facilitates the calculation of this statistic, using the normalized cumulative NDVI data. A Gaussian kernel has been incorporated for spatial weighting, with a designated radius that strategically balances the influence of neighboring pixels against broader spatial influences. This strategy enables efficient calculation of spatial aggregation and dispersion, evaluating the cumulative deviations across the study area to provide a refined assessment of spatial autocorrelation.

Clustering of vegetation gain

Once the trend and cumulative analyses provided insights through visual interpretation of land cover behavior and the mean correlation of the NDVI over time, clustering techniques played a pivotal role in the classification of NDVI pixels across the study area. Utilizing the Google Earth Engine (GEE) platform, the K-means algorithm was employed to segment the landscape into distinct vegetation behavior zones based on NDVI characteristics. This algorithm aids the investigator by grouping large amounts of N-dimensional data into clusters with similar characteristics. The purpose of K-means to simply aid the investigator in obtaining qualitative and quantitative understanding of large amounts of N-dimensional data by providing him with reasonably good similarity groups. Initially the algorithm involves determining a preliminary set of cluster centers (k-means) with a selected value of k. The algorithm proceeds only if the variance within these clusters is above a certain threshold R; clusters with variance below this threshold are not further subdivided. The process initiates with the selection of a preliminary set of cluster centers (k-means) based on a designated value of k. The algorithm then proceeds to refine these clusters, ensuring that only those with within-group variance above a certain threshold, R, are retained and further subdivided. This iterative process continues until the variance within all groups is less than R, thereby ensuring that the clusters are both meaningful and statistically robust. (MacQueen, 1967)

Further refinement in determining the optimal number of clusters was achieved using the training set of random pixels, representing 10 percent of the total in the area, as an input in the NbClust package in R. This package leverages a wide array of indices to recommend the most suitable cluster count, employing both k-means and hierarchical clustering methods across various distance measures, including the Euclidean distance.(Charrad et al., 2014). This number of clusters was then used as a crucial input for the unsupervised classifier, wekaKMeans, which defined the final clusters of changes detected in the study area.

5.5 Other statistical analysis

Considering the region of Agou's location, the climatic conditions conform to a humid tropical ecosystem. According to Piao et al., 2012 , weather conditions such as warming temperatures can influence vegetation growth, obtaining positive results in vegetative cover. Based on this statement, the correlation between precipitation and temperature conditions with vegetation condition variations formed a significant driver to be analyzed.

For the period between 2015 and 2023, temperature and precipitation data were sourced from the Climate Change Knowledge Portal, presented in Celsius degrees (°C) and millimeters (mm), respectively. These climatic variables were integrated as independent factors in a regression model to explore their impact on mean annual NDVI. The model aimed to quantify the influence of each climatic factor by computing coefficients, hypothesizing significant correlations with changes in vegetation observed through NDVI.

5.6 Validation with field data

Field validation is conducted using samples of tree measurements taken in 2021 by the company's own team project. The data included measurements of height, diameter, density, and the names of scientific species taken in the field. Considering that the cluster covers the area, the field samples were compared using the cluster classification layer. Due to the unavailability of the same number of samples per cluster category, a linear mixed-effects model was selected, particularly suited for data that may have non-independence and variability among sample units. In this model, the Fixed Effect includes cluster categories to determine if and how they influence tree height and other vegetative characteristics, while Random Effects account for variations within tree species, acknowledging that different species may respond differently to the same environmental conditions. The analysis utilizes the lme4 package for mixed effects modeling, including the graph and report of the statistical findings.

6 Results and discussion

This section presents the results derived from the applied methodology, including the analysis of NDVI-based metrics, spatial clustering, and statistical assessments. The findings are examined in relation to vegetation recovery trends, afforestation impacts, and potential influencing factors. A comprehensive discussion follows, interpreting the results in the context of the study objectives, previous research, and identified limitations.

6.1 NDVI interpretation and analysis

This section provides a thorough analysis of the results obtained from the comprehensive spatial and statistical analyses conducted to elucidate vegetation dynamics in the Fokpo and Abudjokopé zones from 2016 to 2024. Each analysis subsection is meticulously designed to offer insight into the temporal and spatial vegetative change.

The results obtained provide the first approximation to understanding how vegetation behaviour has changed over time through visual interpretation. Once the calculation of the NDVI was made at the 95th percentile of the Sentinel 2 image data set for the Abudjokopé and Fokpo areas, the visual analysis and interpretation of the results obtained began. The presented graphs are organized by area of interest, with Figure 3 representing Abudjokopé and Figure 4 representing Fokpo. To display the original range values of NDVI from -1 to 1, the symbology selected implements the stretching colors between 0 and 1, using a scale that transitions from brown to green, aiming to focus on only the highest values related to vegetation pixels captured. The values from 0 to 1 indicate that the lowest values represent areas devoid of vegetation or bare soil. This transitions to yellow for areas with very low or barely perceptible vegetation and finally reaches light to dark green, where a value of 1 corresponds to dense vegetation cover. As presented in the NVI transition graphs over time, it is visually perceivable and highlights areas where vegetation cover gains extension or increases density, demonstrating the basis of the project as afforestation activities to recover vegetation cover.

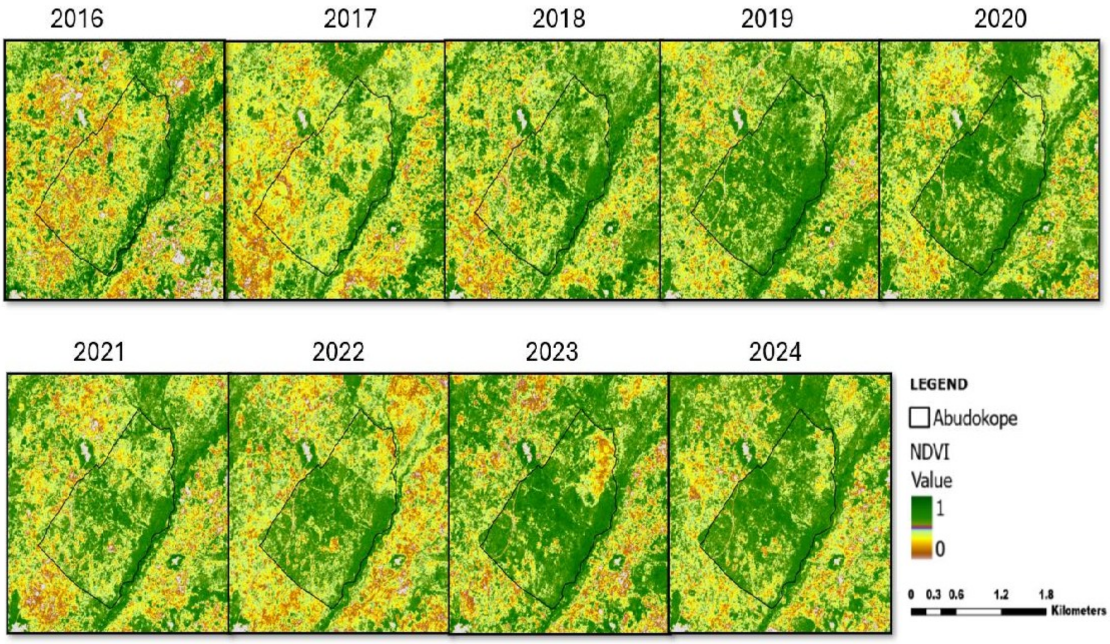

Figure 3. NDVI time series from 2016 – 2024, Abudjokopé zone.

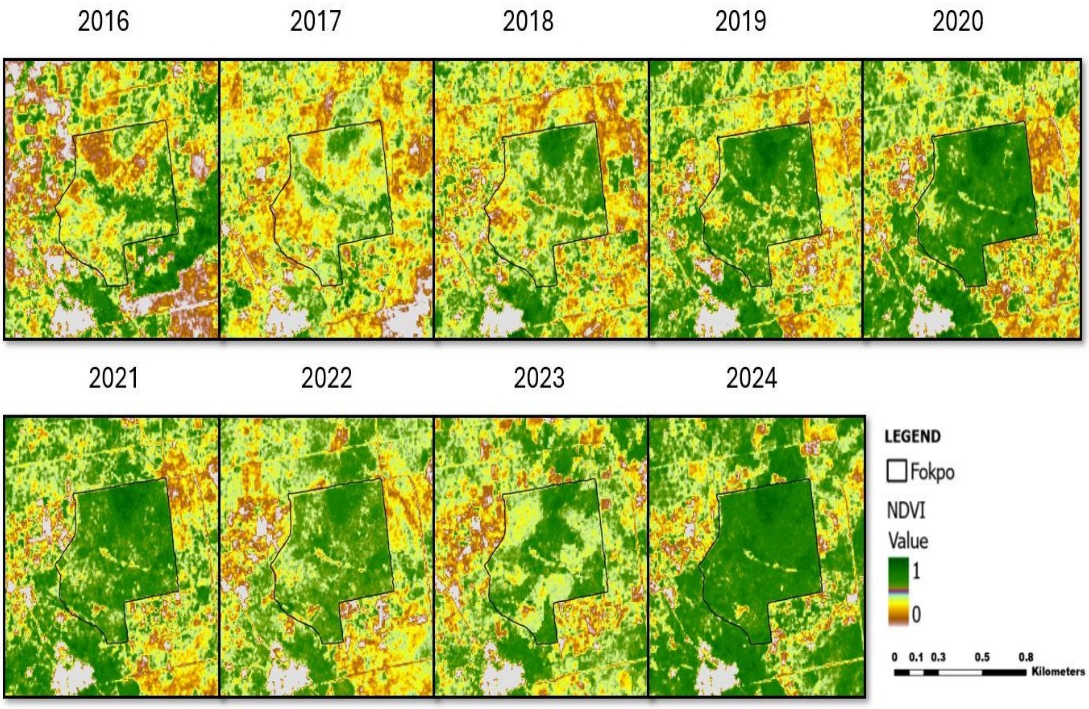

Figure 4. NDVI time series from 2016 - 2024, Fokpo zone.

From a visual inspection, the calculation of the mean NDVI by year highlights that there has been a notable decrease in mean NDVI from 0.698 in 2020 to 0.667 in 2021 and an increase to 0.822 in 2022. This decline in NDVI values during 2021 signifies an anomaly, which, upon fur- ther investigation, was attributed to increased cloudiness and humidity affecting the satellite im- agery capture during this period.

It is evident in such instances that the capacity of satellites to accurately measure surface reflectance can be compromised by atmospheric conditions (Coleman et al., 2024), resulting in potential inaccuracies in NDVI values. Consequently, this can lead to distorted perceptions of vegetation health and cover. Visual results corroborated these findings, highlighting the impact of climatic factors on the reliability of satellite data, and analysis of trend, difference, and cumulative metrics supports the results found.

As demonstrated by the polynomial regression analysis of annual mean NDVI values from 2016 to 2024, the polynomial model reveals a nuanced understanding of the vegetation dynamics detected over the period. Initially, from 2016 to 2020, the model suggests a gradual increase in NDVI, reflecting positive trends in vegetation cover because of an effective natural recovery process in the studied areas. This upward trend is in line with the observed data, which shows an increase from 0.618 in 2016 to 0.698 in 2020. The incorporation of polynomial terms in the re- gression model underscores the intricate nature of vegetation dynamics, particularly by reveal- ing a slight, albeit non-statistically significant, curvature in the trend. This observation signifies the presence of subtle alterations in vegetation health that may not strictly adhere to a linear pro- gression. The model, despite failing to identify significant individual annual trends due to the high p-values of the polynomial coefficients, effectively captures approximately 87.63% of the variability in the data, indicating a reliable model fit.

Following 2021, a decline in the NDVI rate is evidenced; nevertheless, this does not denote a significant or uniform loss of vegetation. One plausible explanation for the observed decline in NDVI is the resumption of afforestation activities in the region, which had been suspended due to the restrictions imposed by the pandemic. This resumption has potentially affected the continuity and effectiveness of fieldwork, contributing to the observed changes in vegetation pat- terns. Furthermore, the decline in the quality of satellite imagery post-2021 may also have influ- enced the observed NDVI trends. It is acknowledged that the present analysis is based on a rela- tively limited timeframe, and further research is necessary to ascertain the long-term implica- tions of these observations.

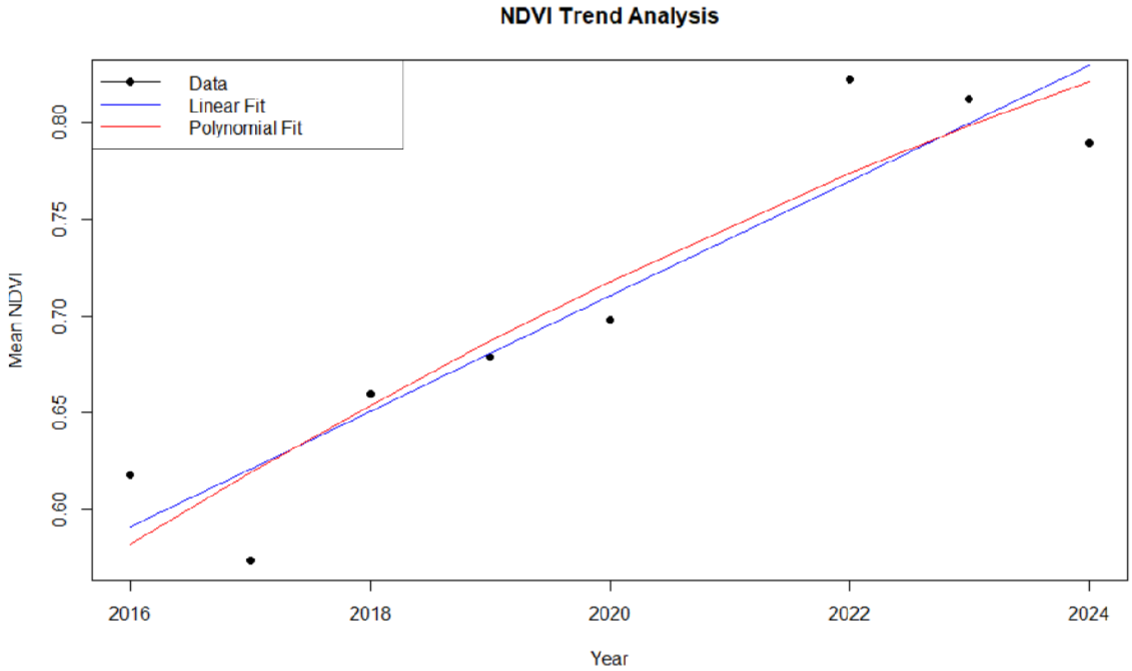

Figure 5. Mean NDVI from 2016 to 2024 in the study area

Linking the trend analysis with the slope values computed in GEE can enhance the understanding of vegetation dynamics over vegetation dynamics over the period. This reveals both increasing and decreasing vegetation tendencies, ranging from -0.018 to 0.050. The negative values express the decreases in mean NDVI values, potentially indicating the degradation. In contrast, the positive values, especially higher than 0, align with the observed increases in the years, particularly in 2022, with 0.05. suggests areas where vegetation health has improved or increased in density, as can be easily captured by the satellite in the red and near-infrared.

To further analyze the vegetation dynamics in the study areas, the cumulative NDVI change offers crucial insights into the temporal and spatial trends of vegetation cover over the period from 2016 to 2024. The cumulative NDVI change, measured from the annual highest-quality pixel values, ranged from a minimum of 2.630 to a maximum of 7.096. This substantial range of 4.466 emphasizes the variability in vegetation health and density within the study areas, suggesting areas of both robust growth and minimal degradation.

Furthermore, the NDVI difference metrics, which demonstrate a minimum and maximum difference of -0.302 and 0.481, respectively, provide additional insight into the year-to-year fluctuations in vegetation health. The areas with the highest values suggest the significant positive change identified in the period, which was the gain of vegetative cover, and negative or lowest values highlight those areas that had not gained vegetation due to the decrease in the value of

NDVI over time. The metrics are crucial for understanding the immediate impacts of annual climatic variations or anthropogenic factors on vegetation, providing a nuanced view of how specific years contribute to overall vegetation trends observed in the cumulative NDVI change data.

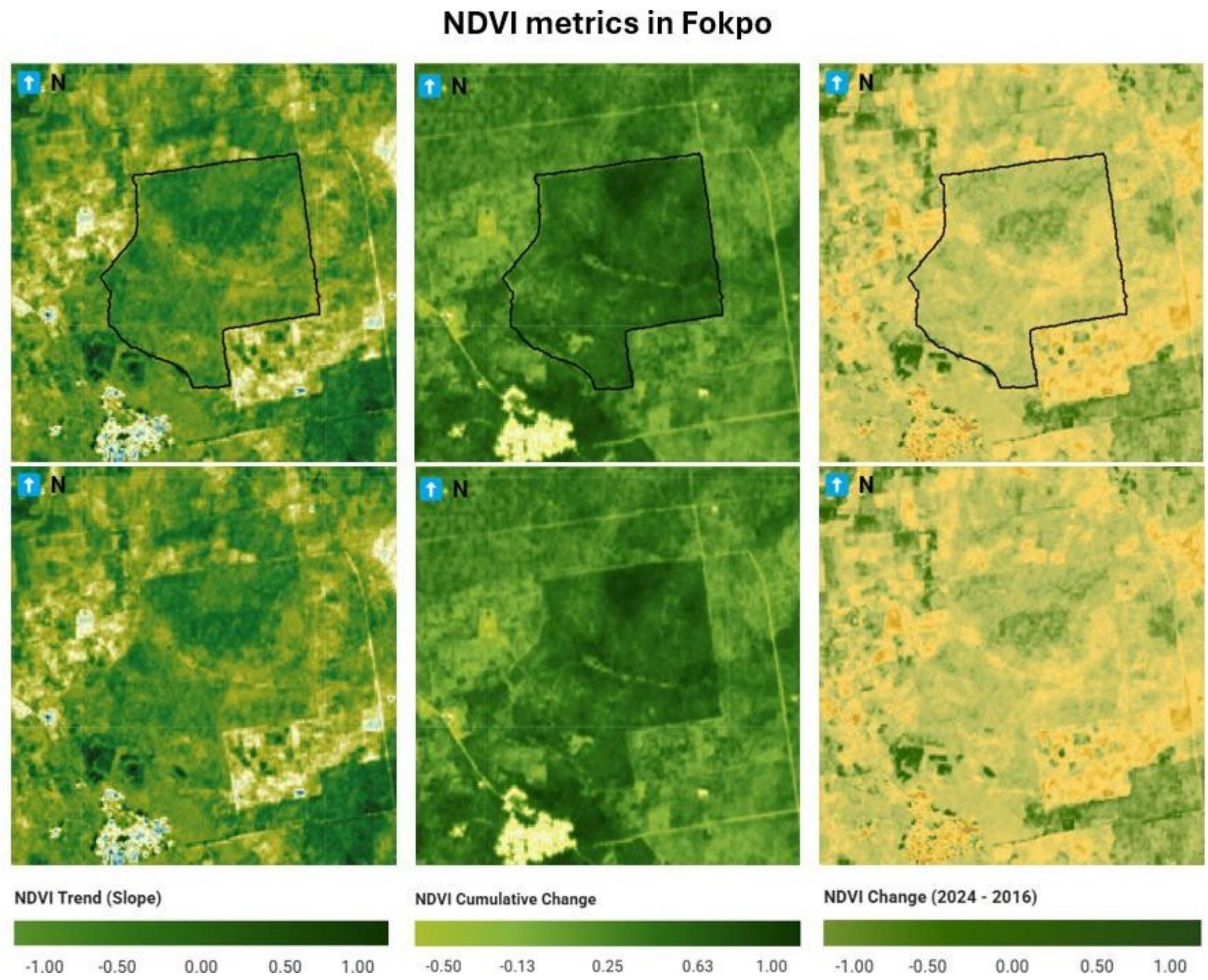

Figure 6. NDVI metrics in Fokpo.

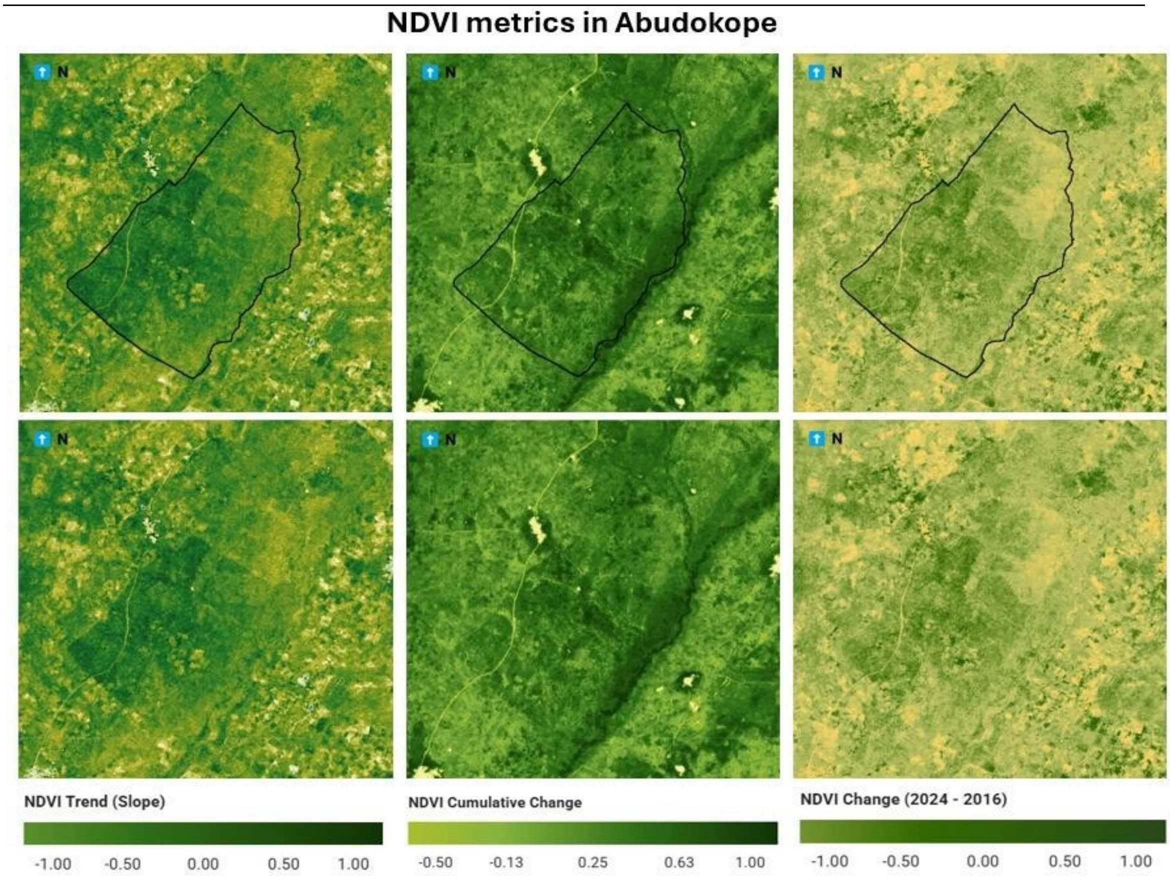

Figure 7. NDVI metrics in Abudjokopé.

6.2 Spatial correlation

The Moran's I univariate index results highlight strong positive spatial autocorrelation within the NDVI data across the Fokpo and Abudjokopé zones, with a normalized value of 0.7258. This statistic, significantly less than one, indicates a moderate to high degree of clustering within the NDVI values. In geographical analysis, such Moran's I values typically suggest that similar NDVI values tend to cluster together rather than being uniformly distributed across the landscape.

This clustering pattern is crucial as it implies that ecological factors influencing vegetation health are not random but are spatially dependent. The fact that the index value does not reach one is significant. It preserves the recognition of spatial heterogeneity within the project area, reflecting the ecological diversity across the study area. This degree of diversity is essential for displaying that some zones observed keep stable, gaining or degrading vegetation.

6.3 Clusters

The NbClust package of R is applied to evaluate the compactness, spacing and density of the clusters. Using the normalization of the features of the 3,000 random pixel sample data with the mean, difference, and trend information of the NDVI of the total area previously obtained in the GEE section of the NDVI metrics.

The K-means clustering algorithm was then applied iteratively across a range of potential cluster numbers, from 2 to 6. This process involved normalizing the feature data of the NDVI to standardize the scale across all variables, enhancing the reliability of the clustering outcomes. A total of 23 different statistical indices were used to assess the multidimensional aspects of cluster validity. These indices provided insights using Euclidean distance to measure dissimilarity between the clusters. The results from the NbClust analysis indicated a significant knee in the plot of the indices, suggesting that 3 clusters provide a meaningful interpretation of the data, as seen in R software report in Figure 8 and Figure 9. This finding is critical as it supports the existence of heterogeneous vegetation behavior zones within the study area.

```
*******************************************************************
* Among all indices:
* 7 proposed 2 as the best number of clusters
* 10 proposed 3 as the best number of clusters
* 4 proposed 5 as the best number of clusters
* 2 proposed 6 as the best number of clusters

                   ***** Conclusion *****

* According to the majority rule, the best number of clusters is  3


*******************************************************************
```

Figure 8.The best number of clusters by R version 4.4.2.

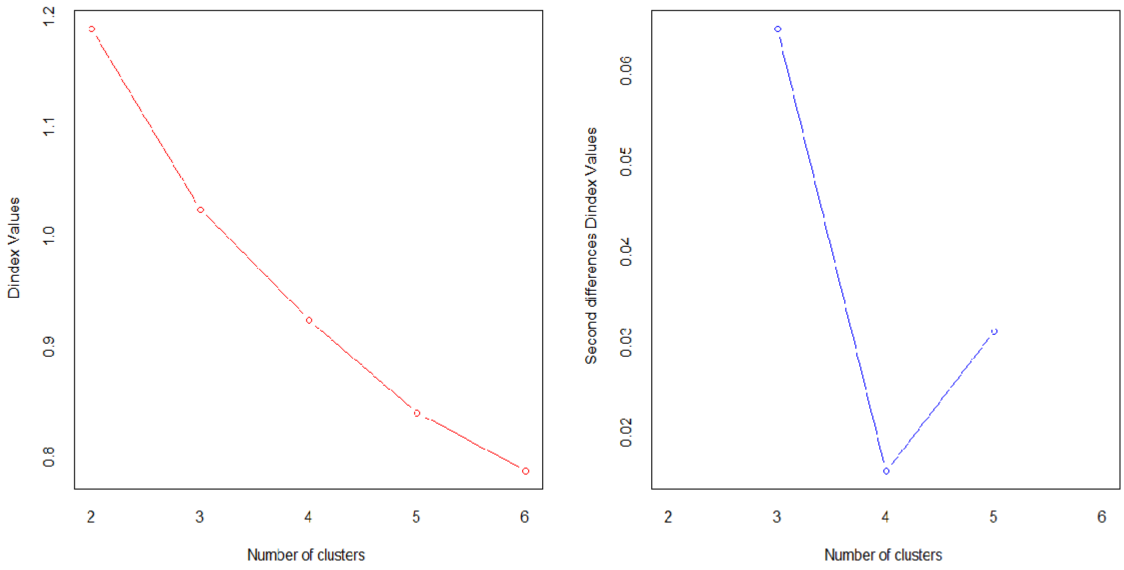

Figure 9. Graph of the best number of clusters by R version 4.4.2.

The results of the *three* number of cluster parameter and the combined NDVI metrics (mean, difference, and trend) for the period 2016-2024 were utilized as input in the classification analysis. The K-means unsupervised classifier clustering algorithm in GEE employed the parameter grouped pixels as 3 to ascertain similarities in their NDVI metrics characteristics pixel value over the study area to obtain the outcome. The classification of clusters is presented in Figure 10 , which is described below:

Cluster 0: Consistently High Vegetation

This cluster is characterized by an average NDVI mean of 0.696, an NDVI difference of 0.112, and a modest NDVI trend of 0.023. The presence of consistently high NDVI readings indicates the presence of stable and robust vegetation at these sites. From the research perspective, the observation of this stability is imperative, as it suggests that these areas could serve as refuges of more stable biodiversity, thereby maintaining ecological balance and serving as benchmarks for assessing the health of surrounding less stable areas. The negligible trend in NDVI change observed in this region could be indicative of a mature, undisturbed state or the success of long-term conservation efforts that have protected these areas from most human impact.

Cluster 1: Significant Transition Vegetation

With an average NDVI mean of 0.716, an NDVI difference of 0.168, and an NDVI trend of 0.029, this cluster signifies regions experiencing more noticeable vegetation growth or recovery. The increase in NDVI values over time is indicative of the efficacy of habitat restoration or natural regeneration processes following a disturbance. The dynamic nature of this cluster underscores the resilience of natural systems when restoration activities are implemented, while also emphasising the critical role of targeted conservation efforts. These areas are of particular value for the study of factors that facilitate vegetation recovery and resilience, providing information that can guide future restoration projects. The monitoring of the evolution of these regions over time can assist in the optimisation of strategies to support ecological recovery in different contexts.

Cluster 2: High Vegetation with Notable Clearings

This cluster exhibits an NDVI mean of 0.701, an NDVI difference of 0.226, and the highest NDVI trend of 0.036, indicating the most dynamic changes within the study areas. It includes zones where significant vegetation cover has transformed from bare soil to grassland or pasture with shrubland, likely in regions that have been the focus of concerted conservation efforts or are naturally recovering from past degradation. The fluctuations in NDVI indicate considerable vegetative disturbance, likely occurring in areas that have experienced intensive conservation efforts or are undergoing natural recovery from prior degradation. This clustering provides a compelling discussion on change and recovery, pointing to which specific interventions may be most effective in fostering such growth. The success of these practices could be replicated in more degraded areas. Additionally, the high variability of this cluster could enhance understanding of the challenges involved in managing highly responsive ecosystems in response to both positive and negative external influences.

The comprehensive NDVI analysis conducted within the Fokpo and Abudjokopé zones has revealed the heterogeneity of vegetation dynamics and highlighted the critical utility of NDVI metrics for monitoring ecological changes. The study has identified specific areas requiring targeted conservation efforts by quantifying these dynamics, thus underscoring the importance of nuanced environmental management strategies. The strong correlation between NDVI differences and trends is particularly revealing, pointing to regions where intervention may be crucial to either mitigate decline or bolster recovery efforts. Insights like these are essential for developing effective conservation strategies that are both adaptable and responsive to the observed ecological conditions.

The results effectively leveraged a combination of quantitative data and visual representations to communicate the complexities of vegetation health and its temporal and spatial variations within the study areas. The presentation of NDVI clustering analysis provides a detailed and actionable understanding of vegetation dynamics, ensuring that the significance of these findings is comprehensively communicated to the reader.

Employing cumulative and differential NDVI metrics has resulted in establishing a robust framework for the analysis of vegetation health, a prerequisite for sustainable management and conservation planning. This approach contributes not only to the scientific understanding of vegetation dynamics but also supports the development of informed policies and practices that can significantly impact ecological sustainability and conservation in the Fokpo and Abudjokopé zones. The findings of this study provide a solid foundation for future research and offer a replicable model for similar ecological studies worldwide, promoting a deeper understanding of how best to manage and preserve our natural environments in an era of rapid environmental change.

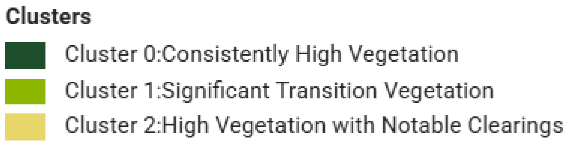

Figure 10. Classification of clusters.

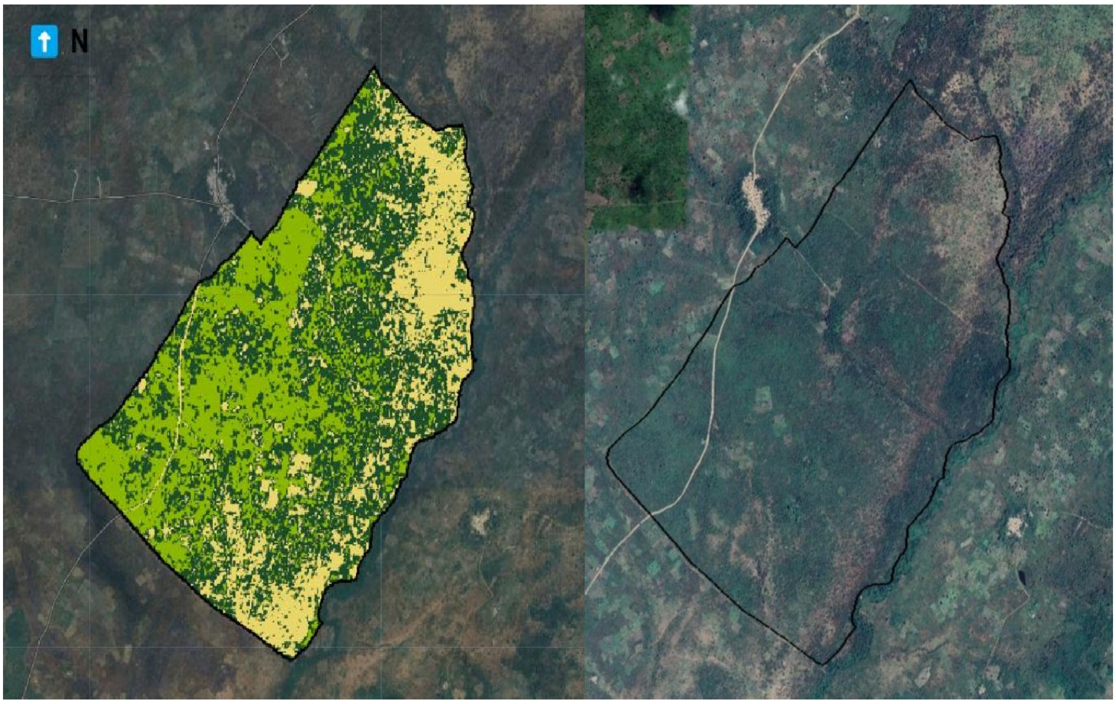

Figure 11. Classification in Abudjokopé.

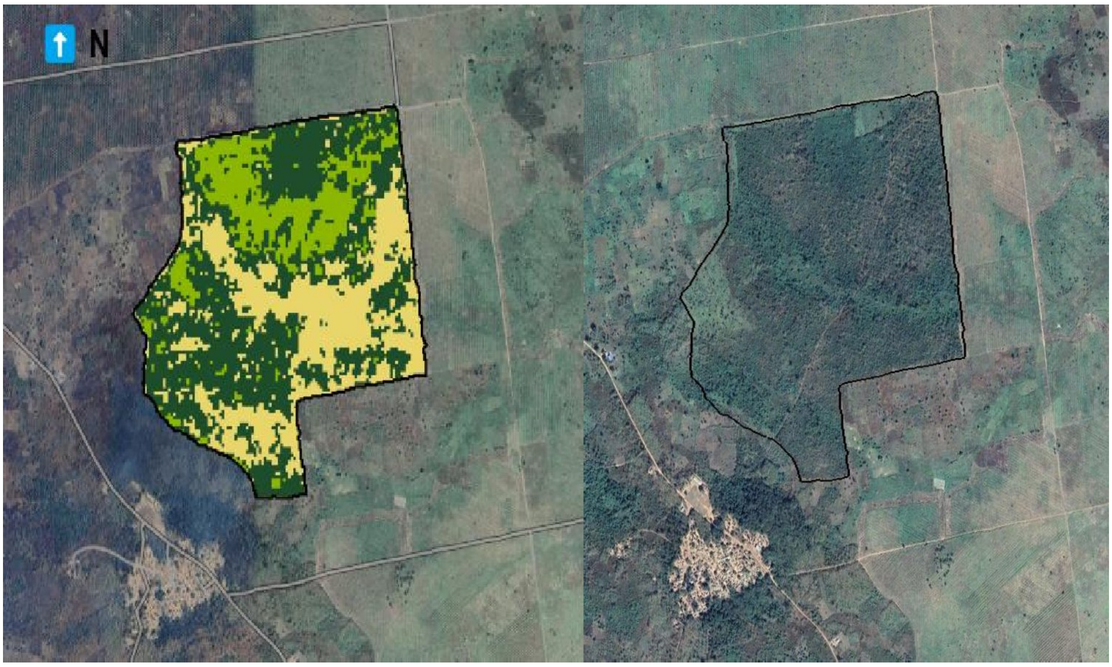

Figure 12. Classification in Fokpo.

6.4 Impact of Climatic Factors on NDVI

The results of the regression analysis revealed that both temperature and precipitation have distinct but statistically non-significant impacts on NDVI. The coefficient for precipitation suggested a slight positive effect, indicating that increases in rainfall could potentially enhance vegetation health, although this was not statistically significant (p-value > 0.05). Conversely, the temperature showed a negative relationship with NDVI, suggesting that higher temperatures might inhibit vegetation growth, also without statistical significance (p-value > 0.05). The model's low R-squared value (0.0429) indicates that only a small portion of NDVI variability could be explained by these climatic variables. This finding suggests that other ecological or non-climatic factors might play more substantial roles in influencing NDVI (Foley et al., 1998; Running et al., 2004). These insights are crucial for developing more targeted environmental management strategies that consider the complex interplay of various climatic and ecological factors.

6.5 Final interphase users

The final script is available on platform GEE; it was developed in a personal academic account; this script includes all the steps highlighted in the Figure 1. Workflow of methodology, in the section 5 Methodology.

And the following Figure 13 display the Workplace available for using the script, the red boxes highlighted each main function with the corresponding label.

- **Script version:** Display the scripts available
- **Full Script:** Include all the steps and lines of code that include the process from consultation NDVI until getting the NDVI layers metrics of Trend, Cumulative, Slope and Final Cluster
- **Execution Script:** The bottom Run allows the user to execute the full script process
- **Map Layers Results:** Display the layers obtained from the script as the red box indicates in this label shows: Study area boundaries (Abudjokopé and Fokpo), NDVI Trend, NDVI Cumulative, NDVI Slope, and Final Cluster.
- **Legend:** The box displays the symbology of each layer available, and the range of values captured by each layer in the case of NDVI Trend, NDVI Cumulative, NDVI Slope, and Final Cluster.
- **Export Data Results:** The script allows the user to export the geographical layers NDVI Trend, NDVI Cumulative, NDVI Slope, and Final Cluster. In addition, export the tables of Cluster statistics, Cluster distribution areas, and the NDVI mean value average per year.

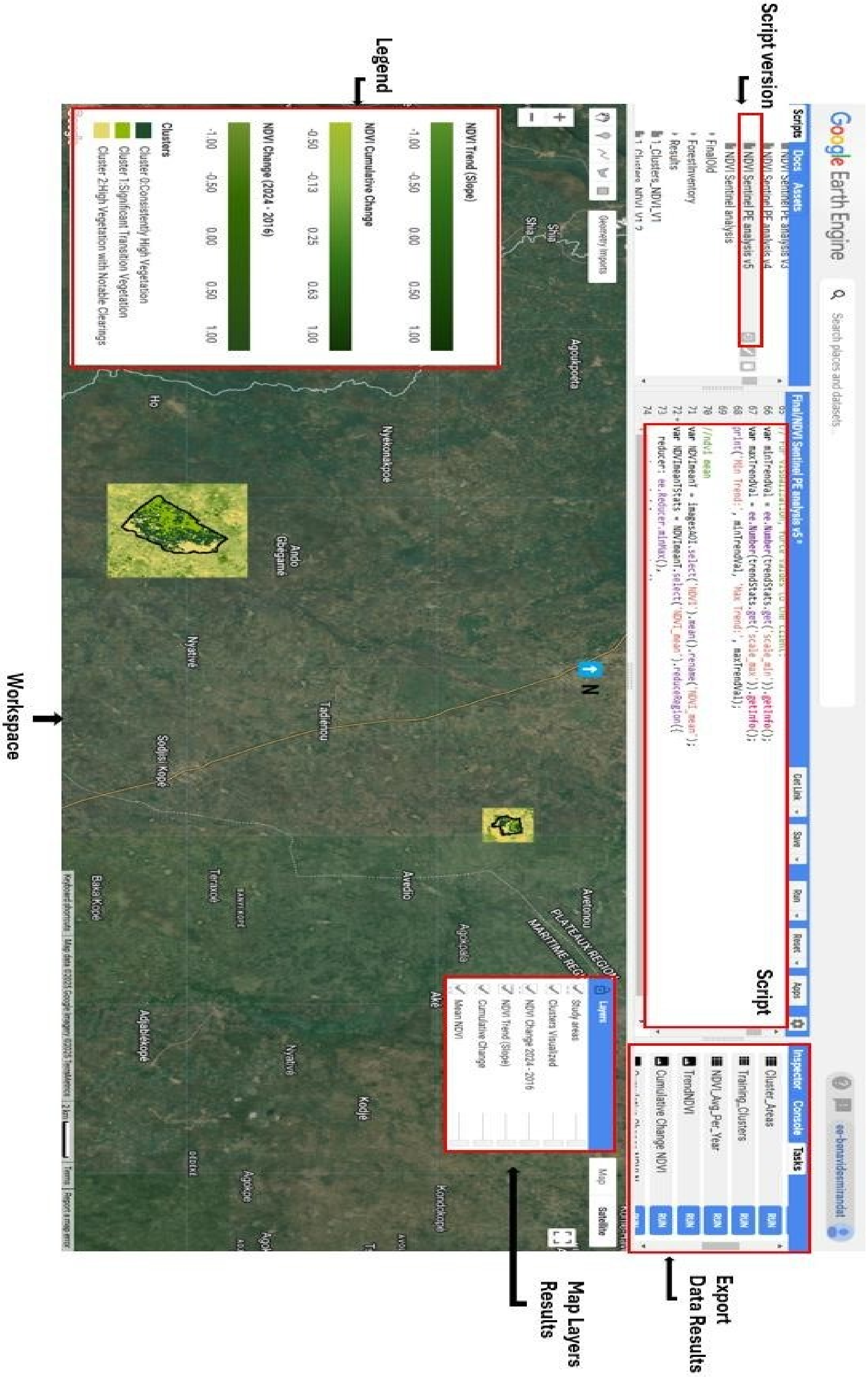

Figure 13. User interface of GEE cluster algorithm for TOGO project study area.

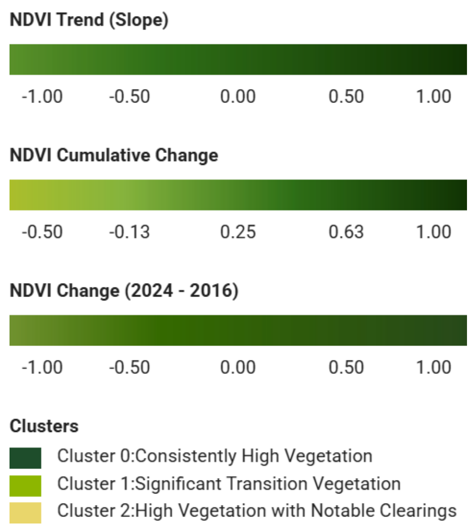

Figure 14. Legend of layers map display.

It is important to mention that the script can be used in any other account without restriction; however, it is necessary to upload the sources from the Area of Study in this research, Abudjokopé and Fokpo in Togo. Once the boundary of the Area of Study is on the platform as an asset, the scripts will run effectively in any other part of the world where Sentinel 2 images are available.

6.6 Field validation of cluster outcomes

The validation of the cluster categories obtained previously was compared with the field data. It could access a group set of samples of field data, which contains information about the tree species, diameter, height, density, and their geographic location in the zone of Abudjokopé. Since only this dataset was available, validation was conducted solely for this zone. The set of data counts 250 grouped in 23 plots where each plot contains 39 different scientific names of tree species, as shown in the following table:

Table 2. Sample trees by Cluster category.

Cluster Category	Number of plots	Number of trees	Number of species
Cluster 0: Consistently High Vegetation	6	72	29
Cluster 1: Significant Transition Vegetation	11	122	31
Cluster 2: High Vegetation with Notable Clearings	6	56	23

Table 3. Physical characteristics of trees average by Clusters.

Cluster	**Density** average	**Diameter (Cm)**	**Height (Mts)**
Cluster 0: Consistently High Vegetation	0.73	14.3	5.4
Cluster 1: Significant Transition Vegetation	0.71	13.9	5.6
Cluster 2: High Vegetation with Notable Clearings	0.74	15.5	6.5

Considering the samples of tree groups by plots are relatively different by cluster category. It selected the linear mixed effect model implemented in the R-provided model, which provides critical insights into how cluster categories influence tree height and how variations among the Scientific Name of species affect these relationships. The statistical outputs indicated through the t-value the significance of each predictor variable.

Cluster 0 - Consistently High Vegetation: The significant negative t-value suggests that trees in this cluster are generally shorter compared to the reference Cluster 2. The effect on tree height varies between -0.6435 ± 0.2784 and the t-value of -2.312 with a negative tendency compared to the reference cluster, indicating stable but less vigorous growth conditions. This may be due to a high but homogeneously spread vegetation density that limits tree height.

Cluster 1 - Significant Transition Vegetation: The slight variation in the effect on tree height, between -0.3277 ± 0.2630 and the negatively trending t-value -1.246, indicates that the trees in this cluster do not reach the heights observed in reference Cluster 2. However, they reflect moderate and continued growth with a small variation from the reference, suggesting a transition zone where vegetation is evolving but not as established as in Cluster 2.

Cluster 2 - High Vegetation with Notable Clearings: This cluster exhibits pronounced growth patterns with significantly taller trees and is set as a reference setting. This represents a hypothetical value t-value of +1.333, where significant positive changes in vegetation health areas are evident. This indicates an area with robust tree growth despite some clearings, reflecting its resilience and dynamic growth conditions.

To the random effects, the model reveals that the scientific name of species characteristics plays a variance of 2.537 and a standard deviation of 1.593 for the interceptions across different species. High variability underscores the substantial influence of species on tree growth through the clusters. However, in conclusion, the inclusion of the scientific name identification of species as a random effect in the model is not merely a statistical consideration but a description of the ecological behavior that does not change significantly through the clusters.

Notable species with better adaptation and relevant tree height by cluster include *Acacia sieberiana DC. var. villosa* in Cluster 0, *Parkia biglobosa* in Cluster 1, and *Anogeissus leiocarpa* and *Pterocarpus erinaceus* in Cluster 2.

The following graph presents the distribution of the diameter and height of the trees found by Cluster; these results, as the previous statistical model, do not identify significant differences between the clusters but allow us to understand the dispersion and variability of physical characteristics by cluster.

Figure 15. Distribution of trees by Cluster category.

Consistently High Vegetation (Green): The trend line demonstrates a strong positive correlation between tree height and diameter, with data points closely clustered around the trend. This tight clustering suggests that trees in this cluster experience stable and uniform growth conditions. The consistency in growth patterns across this group likely reflects a well-established vegetative structure, where trees have reached their optimal growth conditions in an environment with balanced resource availability and minimal disturbance. Such conditions are conducive to maintaining biodiversity and ecological stability, making this cluster an essential area for conservation focus.

Significant Transition Vegetation (Blue): Cluster 1, distinguished by Significant Transition Vegetation, demonstrates a positive correlation between tree height and diameter; however, the data points exhibit a greater variability around the trend line. This increased variability suggests a range of growth rates that varying ecological factors, such as soil fertility, water availability, or recovery stages from disturbances may influence. The larger confidence area around the trend line highlights the uncertainty in growth outcomes, reflecting the transitional nature of this vegetation. Such environments are of critical importance for studying ecological succession and understanding how different species adapt to changing conditions or recover from ecological disruptions.

High Vegetation with Notable Clearings (Red): The graph for Cluster 2 demonstrates a positive correlation between tree height and diameter, though it should be noted that there is significant dispersion among the samples. This variability is higher compared to the other clusters and can be attributed to the heterogeneous nature of the landscape within this cluster. The clearings within the vegetation likely create a patchy environment where light availability and space for growth vary, leading to diverse growth patterns. This cluster, therefore, signifies dynamic ecological zones where disturbances, such as clearings, provide opportunities for new growth and species diversity but also challenge the uniformity of vegetative growth across the area.

7 Conclusions

This study has effectively employed a detection change in vegetative land cover by utilizing satellite images, a vegetation index within the Google Earth Engine (GEE) platform, and supporting statistical analysis in R to monitor vegetation recovery in Togo's afforestation project zones of Abudjokopé and Fokpo over a short period. The results clearly demonstrate a significant enhancement in the capture of vegetation cover in the source, reflecting a positive impact of reforestation efforts.

The meticulous processing of Sentinel 2 imagery, which involved calculating the NDVI for each image annually and selecting the 95th percentile, established distinct patterns of vegetation without biasing the data to a specific section or short timeframe within the year. This approach enabled the identification of vegetation patterns through spatial correlation, where the Moran's I index confirmed significant clustering of vegetation changes. Such clustering suggests that afforestation efforts have been effectively targeted within specific areas of each zone, influencing vegetation dynamics distinctly in Abudjokopé and Fokpo.

The implementation of an unsupervised K-means classifier was pivotal in differentiating between minimal change, moderate transition, and drastic transformation in vegetation. This classification reflects varying degrees of ecological recovery, informed by NDVI metrics such as trend analysis, cumulative values, and slope calculations. The polynomial regression analysis further supported these findings by revealing a generally positive trend in NDVI values, indicating successful vegetation recovery over the study period.

The findings underscore the heterogeneity in vegetation recovery and the effectiveness of targeted reforestation initiatives. A comprehensive analysis of NDVI differences and trends within these clusters yields a more profound understanding of annual and spatial variations in vegetation health. This provides an enhanced perspective on ecological dynamics throughout the study period. Furthermore, the validation process revealed that temperature and precipitation factors did not have a statistically significant impact on the growth rate.

The assessment of field data within the Abudjokopé zone, particularly concerning tree measurements, corroborates the minor differences observed between the clusters, taking into account the plantation activities that commenced around the year 2014. The growth rates of the forest are influenced by the competitive traits of species that exhibit superior adaptability, as well as the pertinent tree height within each cluster. This includes Acacia sieberiana DC. var. villosa in Cluster 0, Parkia biglobosa in Cluster 1, and Anogeissus leiocarpa and Pterocarpus erinaceus in Cluster 2.

In general, the research presented in this thesis provides critical insights into the successes and challenges of reforestation projects within the tropical environmental conditions of the study area. Integrating NDVI analysis with comprehensive statistical and field validation offers a potentially powerful toolkit for monitoring vegetation health and recovery. The findings from this research underscore the potential of integrating NDVI analysis with detailed statistical and field validations as a powerful toolkit for monitoring vegetation health and recovery. This approach not only aids in identifying areas of significant ecological recovery but also highlights zones where vegetation loss or drastic changes require further investigation and intervention.

8 Recommendations for future research

This study provides a structured approach for assessing land cover changes and vegetation recovery using Sentinel-2 satellite imagery and NDVI-based metrics. However, several areas for further research could enhance the accuracy, applicability, and long-term impact of afforestation monitoring.

First, extending the study duration would allow for the analysis of long-term afforestation trends, capturing the full ecological recovery cycle and potential seasonal or climate-driven variations. A longer temporal scale would improve trend analysis and strengthen conclusions on vegetation stability and persistence.

Second, integrating soil and water condition indicators could provide deeper insights into the environmental factors influencing afforestation success. Monitoring soil health, moisture levels, and water availability would help evaluate their role in vegetation recovery and identify potential constraints in afforestation projects.

Third, validating the proposed geospatial model across medium- and large-scale afforestation projects would assess its scalability and adaptability to different ecological and management contexts. Testing the methodology in diverse landscapes and afforestation initiatives would strengthen its robustness and applicability for large-scale conservation planning.

Additionally, implementing the model using high-spatial-resolution satellite data throughout the entire study period would enhance the detection of fine-scale vegetation changes. The use of very high-resolution optical or synthetic aperture radar (SAR) imagery could overcome limitations related to cloud cover and improve the precision of afforestation assessments, particularly in tropical environments.

Lastly, incorporating machine learning and advanced statistical modeling techniques could refine classification accuracy and improve the detection of subtle vegetation changes. The integration of deep learning approaches with Google Earth Engine (GEE) could automate vegetation monitoring, making afforestation assessments more efficient and scalable.

By addressing these research gaps, future studies can enhance the effectiveness of remote sensing-based afforestation monitoring, providing more reliable, scalable, and ecologically meaningful insights for global conservation efforts.

References

1. Amiri, M., & Pourghasemi, H. R. (2022). Mapping the NDVI and monitoring of its changes using Google Earth Engine and Sentinel-2 images. In *Computers in Earth and Environmental Sciences* (pp. 127–136). Elsevier. https://doi.org/10.1016/B978-0-323-89861-4.00044-0

2. Anna. (2024, September 17). *The growing global problem of illegal logging*. Natucate. https://www.natucate.com/en/blog/nature/illegal-logging

3. Barthlott, W., Linsenmair, K. E., & Porembski, S. (2009). *Biodiversity: Structure and function*. Eolss Publishers.

4. Bongers, F., Parren, M. P. E., & Traoré, D. (Eds.). (2005). *Forest climbing plants of West Africa: Diversity, ecology, and management*. CABI Pub.

5. Charrad, M., Ghazzali, N., Boiteau, E., & Niknafs, A. (2014). *An R package for Determining the Relevant Number of Clusters in a Data Set* (Version 62(6)1-36) [R]. https://www.jstatsoft.org/v61/i06/

6. Choudhury, B. J. (1987). Relationships between vegetation indices, radiation absorption, and net photosynthesis evaluated by a sensitivity analysis. *Remote Sensing of Environment*, *22*(2), 209–233. https://doi.org/10.1016/0034-4257(87)90059-9

7. Coleman, R. W., Thompson, D. R., Brodrick, P. G., Dor, E. B., Cox, E., Pérez García-Pando, C., Hoefen, T., Kokaly, R. F., Meyer, J. M., Ochoa, F., Okin, G. S., Pearlshtien, D. H., Swayze, G., & Green, R. O. (2024). An accuracy assessment of the surface reflectance product from the EMIT imaging spectrometer. *Remote Sensing of Environment*, *315*, 114450. https://doi.org/10.1016/j.rse.2024.114450

8. Congalton, R. G. (2001). Accuracy assessment and validation of remotely sensed and other spatial information. *International Journal of Wildland Fire*, *10*(4), 321. https://doi.org/10.1071/WF01031

9. Cortina, J., Maestre, F. T., Vallejo, R., Baeza, M. J., Valdecantos, A., & Pérez-Devesa, M. (2006). Ecosystem structure, function, and restoration success: Are they related? *Journal for Nature Conservation*, *14*(3–4), 152–160. https://doi.org/10.1016/j.jnc.2006.04.004

10. De Beurs, K. M., & Henebry, G. M. (2005). Land surface phenology and temperature variation in the International Geosphere–Biosphere Program high-latitude transects. *Global Change Biology*, *11*(5), 779–790. https://doi.org/10.1111/j.1365-2486.2005.00949.x

11. Dembner, S. A., Nocca-Simmons, Dickerson, R., Burkart, R., Dickerson, N., Phuong, R., Tchamie, J., Dickerson, J., Renoux, & Rollet. (1994). An international journal of the forestry and food industries. In *Unasylva—Parks and protected areas* (Vol. 45). Editorial Advisory Board. https://www.fao.org/4/v2900e/v2900e00.htm#Contents

12. Dos Reis, M., Graça, P. M. L. D. A., Yanai, A. M., Ramos, C. J. P., & Fearnside, P. M. (2021). Forest fires and deforestation in the central Amazon: Effects of landscape and climate on spatial and temporal dynamics. *Journal of Environmental Management*, *288*, 112310. https://doi.org/10.1016/j.jenvman.2021.112310

13. Esri. (2024). *ArcGIS* [Commercial]. ArcGIS. www.esri.com

14. ESRI. (2024). *Esri Deutschland* [Commercial and Academic]. ESRI. https://www.esri.com/de-de/

15. Estimate of vegetation production of terrestrial ecosystem. (2020). In *Advanced Remote Sensing* (pp. 581–620). Elsevier. https://doi.org/10.1016/B978-0-12-815826-5.00015-5

16. European Space Agency, Program of European Union, & Copernicus. (2024). *SentiWiki* [Academic and Commercial]. SentiWiki. https://sentiwiki.copernicus.eu/web/s2-mission

17. FAO. (2025). *Collect Earth, Land & Water* [Agriculture - productivity, Climate, Crops - distribution, Farming systems, Forestry - statistics, Land degradation, Land evaluation, Land use/cover, Remote sensing]. Food and Agriculture Organization of the United Nations. https://www.fao.org/land-water/land/land-governance/land-resources-planning-toolbox/category/details/en/c/1026549/#:~:text=Collect%20Earth%20enables%20developing%20countries,Combat%20Desertification%20(UNCCD)%20and%20United

18. Folega, F., Zhang, C., Zhao, X., Wala, K., Batawila, K., Huang, H., Dourma, M., & Akpagana, K. (2014). Satellite monitoring of land-use and land-cover changes in northern Togo protected areas. *Journal of Forestry Research*, *25*(2), 385–392. https://doi.org/10.1007/s11676-014-0466-x

19. Foody, G. M. (2002). Status of land cover classification accuracy assessment. *Remote Sensing of Environment*, *80*(1), 185–201. https://doi.org/10.1016/S0034-4257(01)00295-4

20. Freden, S. C., Mercanti, E. P., & Becker, M. A. (1974). *Third Earth Resources Technology Satellite-1 Symposium. Volume 1: Technical Presentations, section A*. *Report Number: NASA-SP-351-VOL-1-SECT-A*. https://ntrs.nasa.gov/citations/19740022592

21. Fu, H., Zhao, W., Zhan, Q., Yang, M., Xiong, D., & Yu, D. (2021). Temporal Information Extraction for Afforestation in the Middle Section of the Yarlung Zangbo River Using Time-Series Landsat Images Based on Google Earth Engine. *Remote Sensing*, *13*(23), 4785. https://doi.org/10.3390/rs13234785

22. Galvão, L. S., Breunig, F. M., Santos, J. R. D., & Moura, Y. M. D. (2013). View-illumination effects on hyperspectral vegetation indices in the Amazonian tropical forest. *International Journal of Applied Earth Observation and Geoinformation*, *21*, 291–300. https://doi.org/10.1016/j.jag.2012.07.005

23. Gamon, J. A., Field, C. B., Goulden, M. L., Griffin, K. L., Hartley, A. E., Joel, G., Penuelas, J., & Valentini, R. (1995). Relationships Between NDVI, Canopy Structure,

and Photosynthesis in Three Californian Vegetation Types. *Ecological Applications*, *5*(1), 28–41. https://doi.org/10.2307/1942049

24. Geist, H. J., & Lambin, E. F. (2002). Proximate Causes and Underlying Driving Forces of Tropical Deforestation. *BioScience*, *52*(2), 143. https://doi.org/10.1641/0006-3568(2002)052[0143:PCAUDF]2.0.CO;2

25. Goldman, E., & Weisse, M. (2024, April 4). *World Resources Institute,Top 10 Lists*. World Resources Institute. https://research.wri.org/gfr/top-ten-lists

26. Gorelick, N., Hancher, M, Dixon, M, Ilyushchenko, S., Thau, D., & Moore, R. (2017). *Google Earth Engine: Planetary-scale geospatial analysis for everyone* [Remote Sensing of Environment.]. Google Earth Engine: Planetary-Scale Geospatial Analysis for Everyone. https://earthengine.google.com/

27. Grace, J., Nichol, C., Disney, M., Lewis, P., Quaife, T., & Bowyer, P. (2007). Can we measure terrestrial photosynthesis from space directly, using spectral reflectance and fluorescence? *Global Change Biology*, *13*(7), 1484–1497. https://doi.org/10.1111/j.1365-2486.2007.01352.x

28. Guyot, G., Guyon, D., & Riom, J. (1989). Factors affecting the spectral response of forest canopies: A review. *Geocarto International*, *4*(3), 3–18. https://doi.org/10.1080/10106048909354217

29. Han, W., Li, J., Wang, S., Wang, Y., Yan, J., Fan, R., Zhang, X., & Wang, L. (2022). A context-scale-aware detector and a new benchmark for remote sensing small weak object detection in unmanned aerial vehicle images. *International Journal of Applied Earth Observation and Geoinformation*, *112*, 102966. https://doi.org/10.1016/j.jag.2022.102966

30. Houborg, R., & McCabe, M. F. (2018). Daily Retrieval of NDVI and LAI at 3 m Resolution via the Fusion of CubeSat, Landsat, and MODIS Data. *Remote Sensing*, *10*(6), 890. https://doi.org/10.3390/rs10060890

31. Huete, A., & Justice, C. (1999, April 30). *MODIS VEGETATION INDEX*. University of Virginia. https://modis.gsfc.nasa.gov/data/atbd/atbd_mod13.pdf

32. Huete, A. R. (1988). A soil-adjusted vegetation index (SAVI). *Remote Sensing of Environment*, *25*(3), 295–309. https://doi.org/10.1016/0034-4257(88)90106-X

33. Intergovernmental Panel On Climate Change (Ipcc). (2023). *Climate Change 2022 – Impacts, Adaptation and Vulnerability: Working Group II Contribution to the Sixth Assessment Report of the Intergovernmental Panel on Climate Change* (1st ed.). Cambridge University Press. https://doi.org/10.1017/9781009325844

34. Jin, H., & Eklundh, L. (2014). A physically based vegetation index for improved monitoring of plant phenology. *Remote Sensing of Environment*, *152*, 512–525. https://doi.org/10.1016/j.rse.2014.07.010

35. Kovyazin, V. F., Nguyen, T. A., & Nguyen, T. T. (2023). Monitoring the forest fund lands of Kon Tum province, Vietnam using remote sensing data of Earth. *Geodesy and Cartography*, *998*(8), 57–64. https://doi.org/10.22389/0016-7126-2023-998-8-57-64

36. Lamb, D., Erskine, P. D., & Parrotta, J. A. (2005). Restoration of Degraded Tropical Forest Landscapes. *Science*, *310*(5754), 1628–1632. https://doi.org/10.1126/science.1111773

37. Li, X., Hai, Q., Zhu, Z., Zhang, D., Shao, Y., Zhao, Y., Li, H., Vandansambuu, B., Ning, X., Chen, D., & Liu, Y. (2023). Spatial and Temporal Changes in Vegetation Cover in the Three North Protection Forest Project Area Supported by GEE Cloud Platform. *Forests*, *14*(2), 295. https://doi.org/10.3390/f14020295

38. Liu, L., Zhang, X., Yu, Y., & Guo, W. (2017). Real-time and short-term predictions of spring phenology in North America from VIIRS data. *Remote Sensing of Environment*, *194*, 89–99. https://doi.org/10.1016/j.rse.2017.03.009

39. Lu, D., & Weng, Q. (2007). A survey of image classification methods and techniques for improving classification performance. *International Journal of Remote Sensing*, *28*(5), 823–870. https://doi.org/10.1080/01431160600746456

40. MacQueen, J. B. (1967). *Some Methods for Classification and Analysis of Multivariate Observations.* (Proceedings of the 5th Berkeley Symposium on Mathematical Statistics and Probability, Vol. 1, pp. 281–297). University of California Press. http://projecteuclid.org/euclid.bsmsp/1200512992

41. Major, D. J., Baret, F., & Guyot, G. (1990). A ratio vegetation index adjusted for soil brightness. *International Journal of Remote Sensing*, *11*(5), 727–740. https://doi.org/10.1080/01431169008955053

42. natureOffice. (2025). *TOGO Project*. natureOffice. https://natureoffice.com/en/en-gage/project-togo/natural-forest-afforestation/

43. Olson, D. M., Dinerstein, E., Wikramanayake, D., Burgess, N., Powell, G., Allnutt, T. F., Ricketts, T. H., Kura, Y., Lamoreux, J. F., Wettengel, W., Hedao, P., & Kassem, K. R. (n.d.). *Terrestrial ecoregions of the world: A new map of life on Earth* [Shapefile]. https://www.worldwildlife.org/publications/terrestrial-ecoregions-of-the-world

44. Pettorelli, N., Vik, J. O., Mysterud, A., Gaillard, J.-M., Tucker, C. J., & Stenseth, N. Chr. (2005). Using the satellite-derived NDVI to assess ecological responses to environmental change. *Trends in Ecology & Evolution*, *20*(9), 503–510. https://doi.org/10.1016/j.tree.2005.05.011

45. Piao, S., Tan, K., Nan, H., Ciais, P., Fang, J., Wang, T., Vuichard, N., & Zhu, B. (2012). Impacts of climate and CO2 changes on the vegetation growth and carbon balance of Qinghai–Tibetan grasslands over the past five decades. *Global and Planetary Change*, *98–99*, 73–80. https://doi.org/10.1016/j.gloplacha.2012.08.009

46. QGIS Development Team. (2024). *QGIS Geographic Information System. Open Source Geospatial Foundation Projec* (Version 3.34) [Computer software]. QGIS. http://qgis.osgeo.org

47. Qi, J., Chehbouni, A., Huete, A. R., Kerr, Y. H., & Sorooshian, S. (1994). A modified soil adjusted vegetation index. *Remote Sensing of Environment*, *48*(2), 119–126. https://doi.org/10.1016/0034-4257(94)90134-1

48. R Core Team. (2020). *R: A Language and Environment for Statistical Computing* (Version 4.4.2) [English; X86_64-w64-mingw32/x64]. R Foundation for Statistical Computing. https://www.R-project.org/

49. Ren, H., Zhou, G., & Zhang, F. (2018). Using negative soil adjustment factor in soil-adjusted vegetation index (SAVI) for aboveground living biomass estimation in arid grasslands. *Remote Sensing of Environment*, *209*, 439–445. https://doi.org/10.1016/j.rse.2018.02.068

50. Rouse, J. W. (1973). *Monitoring Vegetation Systems in the Great Plains with ERTS.* (Vol. 1, pp. 309-317.). NASA.

51. Saah, D., Johnson, G., Ashmall, B., Tondapu, G., Tenneson, K., Patterson, M., Poortinga, A., Markert, K., Quyen, N. H., San Aung, K., Schlichting, L., Matin, M., Uddin, K., Aryal, R. R., Dilger, J., Lee Ellenburg, W., Flores-Anderson, A. I., Wiell, D., Lindquist, E., … Chishtie, F. (2019). Collect Earth: An online tool for systematic reference data collection in land cover and use applications. *Environmental Modelling & Software*, *118*, 166–171. https://doi.org/10.1016/j.envsoft.2019.05.004

52. Schneider, A. (2012). Monitoring land cover change in urban and peri-urban areas using dense time stacks of Landsat satellite data and a data mining approach. *Remote Sensing of Environment*, *124*, 689–704. https://doi.org/10.1016/j.rse.2012.06.006

53. Schowengerdt, R. A. (2007). *Remote Sensing*. Elsevier. https://doi.org/10.1016/B978-0-12-369407-2.X5000-1

54. Smelser, N. J., & Baltes, P. B. (Eds.). (2001). *International encyclopedia of the social & behavioral sciences* (1st ed). Elsevier.

55. Song, X.-P., Hansen, M. C., Potapov, P., Adusei, B., Pickering, J., Adami, M., Lima, A., Zalles, V., Stehman, S. V., Di Bella, C. M., Conde, M. C., Copati, E. J., Fernandes, L. B., Hernandez-Serna, A., Jantz, S. M., Pickens, A. H., Turubanova, S., & Tyukavina, A. (2021). Massive soybean expansion in South America since 2000 and implications for conservation. *Nature Sustainability*, *4*(9), 784–792. https://doi.org/10.1038/s41893-021-00729-z

56. The World Bank Group. (2021). *Climate Change Knowledge Portal, For development practitioners and policy makers* [Organization]. The World Bank Group. https://climateknowledgeportal.worldbank.org/country/togo/climate-data-historical

57. Tjøstheim, D., Otneim, H., & Støve, B. (2022). Parametric, nonparametric, locally parametric. In *Statistical Modeling Using Local Gaussian Approximation* (pp. 7–47). Elsevier. https://doi.org/10.1016/B978-0-12-815861-6.00009-2

58. U.S. Geological Survey, & U.S. Department of the Interior. (2024, November 27). *USGS Science for a changing world* [Government]. SGS Science for a Changing World. https://www.usgs.gov/faqs/what-a-geographic-information-system-gis

59. Vitousek, P. M. (1994). Beyond Global Warming: Ecology and Global Change. *Ecology*, *75*(7), 1861–1876. https://doi.org/10.2307/1941591

60. Vrieling, A., Meroni, M., Darvishzadeh, R., Skidmore, A. K., Wang, T., Zurita-Milla, R., Oosterbeek, K., O'Connor, B., & Paganini, M. (2018). Vegetation phenology from Sentinel-2 and field cameras for a Dutch barrier island. *Remote Sensing of Environment*, *215*, 517–529. https://doi.org/10.1016/j.rse.2018.03.014

61. Wagenseil, H., & Samimi, C. (2006). Assessing spatio-temporal variations in plant phenology using Fourier analysis on NDVI time series: Results from a dry savannah environment in Namibia. *International Journal of Remote Sensing*, *27*(16), 3455–3471. https://doi.org/10.1080/01431160600639743

62. Xue, J., & Su, B. (2017). Significant Remote Sensing Vegetation Indices: A Review of Developments and Applications. *Journal of Sensors*, *2017*, 1–17. https://doi.org/10.1155/2017/1353691

63. Yamada, H. (2024). Moran's I for Multivariate Spatial Data. *Mathematics*, *12*(17), 2746. https://doi.org/10.3390/math12172746

64. Yang, Z., Shao, Y., Li, K., Liu, Q., Liu, L., & Brisco, B. (2017). An improved scheme for rice phenology estimation based on time-series multispectral HJ-1A/B and polarimetric RADARSAT-2 data. *Remote Sensing of Environment*, *195*, 184–201. https://doi.org/10.1016/j.rse.2017.04.016

65. Zeng, L., Wardlow, B. D., Xiang, D., Hu, S., & Li, D. (2020). A review of vegetation phenological metrics extraction using time-series, multispectral satellite data. *Remote Sensing of Environment*, *237*, 111511. https://doi.org/10.1016/j.rse.2019.111511

66. Zhang, C., Laurent, S., Sakr, S., Peng, L., & Bédu, S. (2006). Heterocyst differentiation and pattern formation in cyanobacteria: A chorus of signals. *Molecular Microbiology*, *59*(2), 367–375. https://doi.org/10.1111/j.1365-2958.2005.04979.x

67. Zhen, Z., Chen, S., Yin, T., Chavanon, E., Lauret, N., Guilleux, J., Henke, M., Qin, W., Cao, L., Li, J., Lu, P., & Gastellu-Etchegorry, J.-P. (2021). Using the Negative Soil Adjustment Factor of Soil Adjusted Vegetation Index (SAVI) to Resist Saturation Effects and Estimate Leaf Area Index (LAI) in Dense Vegetation Areas. *Sensors*, *21*(6), 2115. https://doi.org/10.3390/s21062115

68. Zoran, M. (2007). *Modeling vegetation reflectance from satellite remote sensing data* (V. I. Vlad, Ed.; pp. 67851J-67851J – 9). https://doi.org/10.1117/12.757871